

Review

A Comprehensive Review of Surface Ozone Variations in Several Indian Hotspots

K. A. Keerthi Lakshmi ¹, T. Nishanth ^{1,*} , M. K. Satheesh Kumar ²  and K. T. Valsaraj ³ 

¹ Department of Physics, Sree Krishna College Guruvayur, Affiliated to the University of Calicut, Thrissur 680102, Kerala, India; keerthilakshmika93@gmail.com

² Department of Atomic and Molecular Physics, Manipal Academy of Higher Education, Manipal 576104, Karnataka, India; drmkssatheesh@gmail.com

³ Cain Department of Chemical Engineering, Louisiana State University, Baton Rouge, LA 70803, USA; ktvalsaraj@gmail.com

* Correspondence: nisthu.t@gmail.com

Abstract: Ozone at ground level (O_3) is an air pollutant that is formed from primary precursor gases like nitrogen oxides (NO_x) and volatile organic compounds (VOCs). It plays a significant role as a precursor to highly reactive hydroxyl (OH) radicals, which ultimately influence the lifespan of various gases in the atmosphere. The elevated surface O_3 levels resulting from anthropogenic activities have detrimental effects on both human health and agricultural productivity. This paper provides a comprehensive analysis of the variations in surface O_3 levels across various regions in the Indian subcontinent, focusing on both spatial and temporal changes. The study is based on an in-depth review of literature spanning the last thirty years in India. Based on the findings of the latest study, the spatial distribution of surface O_3 indicates a rise of approximately 50–70 ppbv during the summer and pre-monsoon periods in the northern region and Indo-Gangetic Plain. Moreover, elevated levels of surface O_3 (40–70 ppbv) are observed during the pre-monsoon/summer season in the western, southern, and peninsular Indian regions. The investigation also underscores the ground-based observations of diurnal and seasonal alterations in surface O_3 levels at two separate sites (rural and urban) in Kannur district, located in southern India, over a duration of nine years starting from January 2016. The O_3 concentration exhibits an increasing trend of 7.91% (rural site) and 5.41% (urban site), ascribed to the rise in vehicular and industrial operations. This review also presents a succinct summary of O_3 fluctuations during solar eclipses and nocturnal firework displays in the subcontinent.

Keywords: air pollution; surface ozone; Kannur; Kerala; India



Citation: Keerthi Lakshmi, K.A.; Nishanth, T.; Satheesh Kumar, M.K.; Valsaraj, K.T. A Comprehensive Review of Surface Ozone Variations in Several Indian Hotspots. *Atmosphere* **2024**, *15*, 852. <https://doi.org/10.3390/atmos15070852>

Academic Editor: Jinqiang Zhang

Received: 31 May 2024

Revised: 11 July 2024

Accepted: 16 July 2024

Published: 19 July 2024



Copyright: © 2024 by the authors. Licensee MDPI, Basel, Switzerland. This article is an open access article distributed under the terms and conditions of the Creative Commons Attribution (CC BY) license (<https://creativecommons.org/licenses/by/4.0/>).

1. Introduction

The rapid growth of industries, urban expansion, and human activities have led to significant deterioration in the quality of the ambient air. The continuous global emission of pollutant gases and particles into the atmosphere causes harm to both human health and the environment. The major air pollutants that are commonly present in the air we breathe daily include particulate matter like PM_{10} and $PM_{2.5}$, nitrogen oxides ($NO_x = NO + NO_2$), sulphur dioxide (SO_2), surface ozone (O_3), methane (CH_4), non-methane hydrocarbons (NMHCs), carbon monoxide (CO), and volatile organic compounds (VOCs) [1,2]. Air pollution is primarily caused by industrial activities, vehicle emissions, agricultural practices, and natural phenomena such as wildfires and volcanic eruptions [3].

Atmospheric O_3 (stratospheric and tropospheric) plays a pivotal role in maintaining ecosystems on the earth's surface. O_3 can be either good or bad depending on where the O_3 is and its concentration. Approximately 90% of the O_3 in the atmosphere is located in the stratosphere, with the remaining 10% found in the troposphere [4]. The rather limited quantity of tropospheric O_3 serves as a significant greenhouse gas, posing a threat to both

biological life and plant species due to its increasing trend [5]. Myhre [6] reports that O₃ is identified as the third most significant trace gas in the total tropospheric radiative forcing (RF) since the pre-industrial era. The increase in O₃ levels has resulted in a worldwide radiative forcing of +0.35 Wm⁻², causing a notable impact on climate change.

Despite its minor presence, tropospheric O₃ plays a critical role in atmospheric chemistry and the oxidising capacity of the atmosphere [7]. As a result, O₃ is recognized as a significant trace gas in the troposphere that can greatly impact atmospheric chemistry [8]. The International Global Atmospheric Chemistry Project (IGAC) has developed the Tropospheric Ozone Assessment Report (TOAR-I and II) to answer questions such as which regions have the most O₃ pollution in the world, how much O₃ concentration is increasing in developing countries, and what the effects are of O₃ on ecosystems [9–13]. Based on the report, tropical locations in India are the most polluted regions with a greater availability of O₃ profiles compare with Western Africa, the tropical South Atlantic, Southeast Asia, Malaysia, and Indonesia [14]. Data from ozonesonde and aircraft observations indicate that the global O₃ distribution in the 21st century surpasses that of the 1970s and 1980s [15].

The major sources of surface O₃ are the photochemical production and transport from the stratosphere [16]. The abundance of surface O₃ can be greatly affected by variations in the concentration of precursor gases (NO_x, CH₄, CO₂, NMHCs, and VOCs), photochemical reactions, and local weather conditions. Moreover, the daily and seasonal variations in O₃ are significantly influenced by changes in atmospheric temperature, relative humidity, wind speed, and the long-range transport of air mass [17–19]. Change in surface O₃ and meteorological factors have been extensively monitored in the urban area of the northern hemisphere, especially in North America and Europe [20–22]. With slight variation throughout the year, surface O₃ concentration has increased since the 19th century from about 10 ppbv at mid-latitudes over Europe and 5 ppbv in tropical regions [23]. Hence, it is imperative to conduct a comprehensive analysis of long-term fluctuations of meteorological parameters in order to investigate the chemical composition of surface O₃ at a specific geographical area [24].

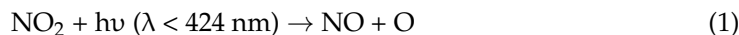
Various studies have been accomplished on the photochemical production of surface O₃ from its precursor gases over different parts of the globe [25–52]. The results of these investigations indicate that elevated levels of O₃ are detected during the summer and pre-monsoon periods. This phenomenon is mainly ascribed to heightened photochemical reactions and the inflow of O₃ from the stratosphere. High altitude sites (Mt. Fuji and Mauna Loa) show a springtime maximum O₃ concentration which is mainly explained on the basis of downward transport of O₃-rich air from higher altitudes [53,54]. Conversely, lower concentrations of O₃ are observed during the monsoon season, which can be attributed to the presence of wet weather conditions.

The increase in temperatures caused by heat waves has intensified the generation of surface O₃, leading to a decline in air quality in numerous regions worldwide [55–57]. As research advanced, concerns mounted among scientists regarding the detrimental effects of surface O₃ on human well-being, agricultural yields, air quality, and ecosystems [58,59]. Consequently, government authorities and environmental organizations around the globe have implemented strategies to control the release of O₃ precursors and reduce surface O₃ concentrations. These efforts have included regulations on vehicle emissions, industrial practices, and programs to monitor air quality.

This study illuminates the spatial and temporal fluctuations of surface O₃ levels across various regions within the Indian subcontinent. Our aim was to conduct a thorough examination of the vast array of research conducted in India over the last thirty years. Additionally, the research highlights the daily and seasonal variations in surface O₃ concentrations recorded at two specific locations in the Kannur district of southern India, spanning a period of nine years from January 2015. The subsequent section will delve into a concise overview of the formation of O₃ at ground level, originating from its key precursors and the accompanying chemical reactions.

2. Photochemical Production of Surface O₃

The surface O₃ formation is generally initiated by the photolysis of NO₂. In the presence of solar radiation, NO₂ undergoes photolysis to produce NO and atomic oxygen and this atomic oxygen reacts with O₂ to produce O₃.



There are no significant sources of O₃ in the surface level other than reaction (2). The O₃ produced from this reaction rapidly reacts with NO to form NO₂.



2.1. Role of CO and VOCs on Surface O₃ Formation

The hydroxyl radical is the key reactive species in the chemistry of O₃ formation. At a high ratio of VOC to NO_x concentration, OH will react mainly with VOCs; at a low ratio, the NO_x reaction can predominate. CO reacts with OH, forming H atoms that are quickly scavenged by O₂, yielding the hydroperoxyl radical (HO₂).



Hydroxyl (OH) also outbreaks hydrocarbons (RH), and other VOCs, leading to alkylperoxy radicals (RO₂):



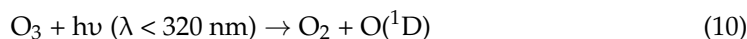
HO₂ and RO₂ oxidize NO to NO₂, reforming OH:



This NO₂ generates more O₃, within, typically, 1 to 2 min.

2.2. Photochemical Destruction of Surface O₃

The photochemical loss of O₃ occurs in the lower atmosphere as a part of a series of reactions by which primary pollutants such as hydrocarbons and nitrogen oxides react to form secondary pollutants such as peroxyacetyl nitrates



which generates an excited oxygen atom O(¹D), which can react with water to give hydroxyl radical (OH)



The hydroxyl radicals are central to atmospheric chemistry as they initiate the oxidation of hydrocarbons in the atmosphere and so act as a detergent. In remote regions, O₃ is also consumed by reactions with HO₂ and OH



An additional loss of O₃ takes place by dry deposition at the Earth's surface. Dry deposition, in general, refers to the transport of gaseous and particulate species from the

atmosphere onto the earth's surface in the absence of precipitation. For trace gases, the solubility and chemical reactivity may affect the uptake at the surface [60].

3. Surface O₃ Measurements in India

Though India is experiencing rapid economic growth, this progress is accompanied by a significant air pollution problem throughout the country. In the north-eastern region of the country, there is a noticeable increase in tropospheric O₃ levels, largely due to industrial and anthropogenic activities. Factors such as active biomass burning, high temperatures, and dry weather in the summer season contribute to the formation of tropospheric O₃. Observations and model simulations have revealed a significant rise in O₃ concentrations in the industrial cities like Delhi, Kanpur, Ahmedabad, Hyderabad, and Bangalore, all of which are experiencing increased anthropogenic activities. Research on surface O₃ in India began around thirty years ago and it is currently ongoing at more than 20 different sites across the nation.

Various institutions such as the National Environmental Engineering Research Institute (NEERI), the Indian Institute of Tropical Meteorology (IITM), laboratories under the Council of Scientific and Industrial Research (CSIR) and Indian Space Research Organizations (ISRO), the Indian Institute of Technologies (IITs), the Indian Institute of Science (IISc), and the Indian Institute of Science Education and Research (IISER) have been actively involved in monitoring the surface O₃ levels. These establishments have made use of ground and space-based observations, in addition to suitable models, to verify their findings and evaluate the origins and effects of surface O₃. The Ministry of Earth Science (MoES), Government of India, has installed automatic weather stations in each district throughout India to secure the availability of high-resolution spatial and temporal data on meteorological parameters. These stations are integrated into national networks situated in major cities and industrial zones, with the goal of monitoring the influence of meteorological parameters on surface O₃ concentrations and ensuring compliance with national air quality standards.

3.1. Concise Overview in the Indian Region

Followed by China and the United States, India is the third largest emitter of greenhouse gases globally [61]. The country is facing a significant environmental challenge due to surface O₃ pollution, particularly in urban and industrialized areas with high levels of O₃ precursor emissions. Over the last thirty years, the measurements of O₃ across the Indian subcontinent have shown a significant rise at the surface level. North India and its surrounding areas are considered the global hotspots for air pollution. Therefore, continuous ground-based observations of trace pollutants are being conducted in north India and the Indo-Gangetic Plain [62–66].

Kumar [67] conducted a study that revealed a daily variation in surface O₃ levels at the same location (Nainital). They also observed a distinct seasonal trend, with the highest O₃ concentration typically observed in late spring, sometimes surpassing 100 ppbv, and the lowest levels during the monsoon season. Through the examination of air trajectories and model simulations, it was determined that stratospheric transport significantly impacts O₃ levels in Nainital in comparison to local pollution. Sarangi [68] conducted a study on O₃, CO, and NO_y in Nainital, a hill station in the Himalayas. The study revealed that while O₃ levels remained stable, there was an increase in CO and NO_y levels during the daytime. These fluctuations were associated with atmospheric dynamic processes, including vertical winds and the formation of a strong boundary layer over the Himalayas.

Harithasree [69] carried out on-site measurements of surface O₃ attributes in the Doon valley of the Himalaya region from April 2018 to June 2023. The results of the study revealed that O₃ levels peaked at noon throughout the year, with the highest concentration occurring in the pre-monsoon period and the lowest during winter and monsoon seasons. This research also highlighted that the photochemical generation of O₃ occurs in the transition or VOC-limited regime, emphasising the significance of decreasing emissions of NO_x and

volatile organic compounds to address surface O₃ pollution. Soni [70] found that despite the low levels of primary pollutants in Ahmedabad, there was a significant increase in surface O₃ during the lockdown period. Using model simulations, they revealed that this rise was due to changes in meteorological conditions and atmospheric chemistry. Additionally, their research emphasized the complex relationship between emission reductions, intricate chemical reactions, and meteorological variations in influencing O₃ concentration.

An investigation was conducted by Kumar [71] to examine the influence of VOCs and OH radicals on the chemical reactions involving surface O₃ in the north-western part of India. The results of their research indicated that both NO_x and VOCs have a substantial impact on regulating the formation of surface O₃ in the Indo-Gangetic Plain. Moreover, it was also discovered that isoprene and acetaldehyde produced as a result of human-made and natural emission sources, play a crucial role in O₃ production. This impact remains significant throughout the entire year.

Nelson [72] carried out an innovative study to examine the impact of VOCs on surface O₃ formation in Delhi using the Master Chemical Mechanism model. The research focused on investigating the sensitivity of VOCs' influence on local O₃ production rates within a VOC-limited chemical environment in Delhi during periods of smog. Tyagi [73] carried out an investigation into the surface levels of O₃ and NO_x in three distinct locations within the north-eastern region of India, specifically Aizwal, Guwahati, and Tezpur in the year 2016. The results indicated that Tezpur, situated in a valley in the Himalayas, displayed elevated concentrations of both O₃ and NO_x in comparison to the other two sites. Notably, all three sites experienced peak levels of O₃ and NO_x during the pre-monsoon period. This occurrence was linked to the extensive transport of pollutants from the Indo-Gangetic Plain, as well as the industrial zones in Jharkhand, Odisha, and West Bengal.

Hama [74] analysed the spatio-temporal features of particulate matter and trace gases within a network of 12 air quality monitoring stations throughout Delhi-NCR from 2014 to 2017. It was discovered that the levels of air pollutants, excluding surface O₃, were notably elevated during the winter season compared to the monsoon and summer seasons. Additionally, they noted that O₃ concentration exhibited the highest variation in summer and the lowest in winter. Dumka [75] conducted research on the fluctuations of O₃, NO_x, CO, CH₄, and NMHCs in Guwahati, located in the Brahmaputra river valley of north-eastern India. Their findings revealed that surface O₃ exhibited the highest levels during the pre-monsoon and winter seasons due to seasonal variations. Additionally, they identified that the emission of local NO_x from the nearby national highway significantly contributed to the rise in O₃ levels at the monitoring station.

The study by Kanchana [76] focused on the meteorological factors and fluctuations in surface O₃, NO_x, CO, and black carbon (BC) in Hyderabad between 2016 and 2017. It was discovered that O₃ levels were elevated in winter and decreased during the monsoon season. Moreover, the investigation emphasized the impact of the Atmospheric Boundary Layer (ABL) height on the concentrations of O₃ and BC. The investigations conducted by Yadav [77] in Udaipur during 2011–2012 found that the pre-monsoon season had the highest surface O₃ levels as a result of convective activities. A significant impact of variations in planetary boundary layer (PBL) height and meteorological changes on the variation in O₃ and other pollutants was detected.

Bhardwaj [78] observed the fluctuations in surface O₃ and its precursors across Bode in Nepal, as well as two neighbouring sites in Nainital and Pantnagar located in the central Himalayan regions of India. They discovered a significant negative correlation between surface O₃ and CO at these locations. Pancholi [79] conducted a study in Jodhpur to investigate the seasonal and diurnal behaviour of surface O₃ and NO_x. The research findings showed notable variations in both daily and seasonal levels. Through an analysis of O_x and NO_x levels, the researchers aimed to understand the oxidative dynamics in the region. The results emphasized the significant contributions of air pollutants from both local and regional sources, vehicular exhaust being a major factor.

Mahapatra [80] investigated the different physical and chemical mechanisms that led to an unusual decrease in surface O₃ levels in Bhubaneswar during December 2010. They conducted simulations using WRF-Chem and analysed various factors such as meteorological parameters and backward air trajectories on in situ surface O₃ variations. Their findings revealed that the reduced O₃ concentration was primarily influenced by the transportation of cleaner marine masses to the observation site due to a rare low-pressure event. Saini [81] conducted a study on the variation in surface pollutants at a traffic junction in Agra. Their investigation revealed an increased level of surface O₃ during the summer season. Additionally, they observed an elevated concentration of NO₂ and CO mixing ratios at the observational site during the post-monsoon and winter seasons.

Yadav [82] reported that the highest mixing ratios of surface O₃ occur during the winter/pre-monsoon season in Udaipur. They found that the diurnal variation in O₃ over Udaipur is significantly influenced by the temporal changes in local emissions and the variation in ABL height. The study also emphasized the elevated levels of O₃ during the afternoon hours, which were attributed to the increased photochemical production and the intrusion of air from the free troposphere. Sharma [83] observed a distinct seasonal fluctuation of trace gases in their study on surface O₃ and its precursor gases at an urban site in Delhi. The levels of O₃, NO_x, CH₄, and NMHC were found to be highest during the summer, while CO exhibited higher concentrations during the winter season. Additionally, the analysis of PM and O₃ revealed that the concentration of PM in the surrounding air has a significant impact on the production of surface O₃ in Delhi.

Tyagi [84] conducted a study on gaseous pollutants in seven distinct regions of Delhi. Their observations revealed that during noontime, there is a significant presence of O₃ due to the increased photochemical activities. Additionally, they noted that the concentrations of CO are influenced by the dynamics of the nocturnal boundary layer. An investigation conducted by Mallik [85] focused on analysing the fluctuations in surface O₃ levels and its precursors in Ahmedabad. The study revealed that the spontaneous increase in trace gas levels during the post-monsoon period is attributed to shifts in wind patterns. Additionally, the researchers observed a distinct correlation between the concentrations of CO, NO_x, and SO₂ and the direction of wind, which varied based on the emission sources.

During the period from August 2005 to March 2007, Mandal [86] conducted a study to examine the fluctuations in surface O₃ and its precursor gases at Port Blair, a secluded marine station located in the Bay of Bengal. The researchers identified elevated levels of O₃, NO_x, and CO in the months of March and November. These heightened concentrations were due to the transportation of pollutants over long distances from the eastern region of the Indian subcontinent. Using balloon-borne sensors, Lal [87] found an elevated level of O₃ in Ahmedabad from April to June. Their research revealed that O₃ levels are mostly varying in the upper troposphere, its fluctuations being influenced by its movement from the stratosphere.

Ojha [88] explored the vertical distribution of O₃ above Nainital through the use of ozonesonde. Their findings indicated that the highest O₃ levels are observed during the spring season, with the likelihood of stratospheric intrusion in the winter season, resulting in an increased O₃ concentration in the middle-upper troposphere of Nainital. Moreover, they highlighted that the surge in O₃ levels is predominantly caused by regional pollution in the Indo-Gangetic region along with biomass burning in northern India. During the years 2009–2011, Ojha [89] conducted a study to examine the variations in surface O₃ levels in Pantnagar, a semi-urban area located in the Indo-Gangetic Plain (IGP) region. Their findings revealed that the daytime accumulation of O₃ concentrations reached a peak of 100 ppbv. These changes in concentrations were found to have an impact on emissions and photochemical processes in the IGP region, consequently affecting the air quality in the Himalayan region. The MATCH-MPIC model simulations indicated that the observational site operates under a NO_x limited regime.

Mahapatra [90] investigated the seasonal fluctuations and health hazards linked to the levels of gaseous pollutants in the atmosphere of Bhubaneswar from December

2010 to November 2012. They observed elevated levels of surface O₃ and CO during the winter months, due to increased regional emissions and the long-range transport of pollutants from the Indo-Gangetic Plain to the monitoring location. Bhuyan [91] carried out research investigating the impact of precursor gases and meteorological conditions on the fluctuations of O₃ levels in Dibrugarh, situated in the Himalayas within the Brahmaputra basin. Their findings revealed high concentrations of O₃ levels in March as a result of the emission of pollutants within the local area.

Gaur [92] observed the fluctuations of trace gases in Kanpur over a span of four years. Their findings revealed that trace pollutants, with the exception of surface O₃, exhibited peak concentrations during the winter season, while O₃ reached its highest levels during the summer months. Swamy [93] conducted a study on the impact of precursors and Black Carbon on surface O₃ concentrations at a semi-arid urban site in Hyderabad. The research findings highlighted the significant contribution of local emissions of trace pollutants and meteorological parameters in shaping the daytime variations in surface O₃. Interestingly, the study also revealed that O₃ concentrations were higher on weekends compared to weekdays, with the impact being particularly pronounced during the winter season.

Reddy [94] conducted an observational study on ground level O₃ in Anantapur from 2008 to 2009. Their investigation revealed distinct diurnal and seasonal variations, highlighting the highest rate of O₃ production occurs in March, while the lowest rate is observed in July. Singla [95] conducted a study on the levels of surface O₃ and its precursor at Dayalbagh, Agra during 2008–2009. The findings of the study indicated that the maximum concentration of O₃ during the day was observed between 12:00 and 14:00 h, which can be attributed to photochemical production. The study also revealed that O₃ levels exhibited significant seasonal variations, with higher concentrations observed during the summer and winter seasons, and lower concentrations during the monsoon and post-monsoon seasons.

Debaje and Jeyakumar [96] investigated the fluctuations in surface O₃ levels at five different sites along the west coast of the Bay of Bengal. Their research found that the concentration of O₃ is higher at the shoreline compared to 20 km inland. They attribute this elevated O₃ concentration in the coastal area to the presence of chlorine species, which are produced from the organic reaction of sea salt elements with a lifetime of less than 10 min. Also Debaje and Kakade [97] examined the variations in surface O₃ levels at five distinct locations in western Maharashtra from 2001 to 2005. Their results showed a significant seasonal fluctuation in O₃, with a notable peak during the summer and winter seasons at both urban and rural sites. The study also indicated that local pollutants played a crucial role in increasing O₃ concentrations at the urban and rural sites, while local transport had a significant impact in high altitude mountainous areas.

Ghude [98] investigated the variation in surface O₃ concentration in Delhi for seven years and found that the levels of O₃ on the ground in the city surpass the “critical levels” considered safe for human health, vegetation, and forests. They also discovered that the concentration of O₃ levels significantly increased above 40 ppbv during the winter and pre-monsoon seasons in Delhi. Beig [99] observed a peak in surface O₃ levels during 2003–2004 in Pune at noontime. They found that the concentration of O₃ was impacted by pollution transported regionally or over long distances to the observation site.

The study conducted by Naja [100], on surface O₃ levels at the high altitude location of Mt. Abu from 1993 to 2000, revealed that O₃ concentrations are at their lowest during daytime hours. The diurnal pattern of O₃ levels significantly changes after the northeast monsoon period. Furthermore, it was observed that the pollutants present in the local area are the main factors leading to the observed elevated concentration of O₃ in the late autumn and winter season. Another investigation by Naja [101], at Gadanki, on the variation in surface O₃ and precursor gases from 1993 to 1996, revealed a minimal correlation between O₃ and NO_x. This suggests that the levels of NO_x in Gadanki are not regulated by combustion or emissions, but could be attributed to transportation from nearby major towns.

Lal [102] conducted measurements of surface O₃ and its precursors in Ahmedabad from 1991 to 1995. The findings indicate that the daytime accumulation of O₃ was primarily a result of the photo-oxidation of precursor gases. Variations in ABL height, surface wind patterns, and meteorological parameters also play a key role in regulating the daily fluctuations of trace pollutants in Ahmedabad. In terms of long-term analysis, the study revealed that the seasonal variation in O₃ was the highest during the winter–spring season in 1954–1955, whereas in 1991–1995, the highest concentration was observed during winter–autumn season. This disparity in seasonal variations suggests that solar radiation previously controlled the seasonal variation, whereas now it is predominantly influenced by local and regional pollutants.

Sai Krishnaveni [103] conducted a thorough analysis on the spatio-temporal correlation between particulate matter and surface O₃ in four urban locations (Delhi, Bengaluru, Ahmedabad, and Kolkata) and a rural area (Gadanki) in India. The study utilized data from various sites across India spanning a 4-year timeframe (2019–2022). The findings of the study revealed that meteorological factors significantly influence the relationship between PM_{2.5} and O₃ in rural regions. Moreover, within urban areas, emission sources and atmospheric chemistry are more influential in shaping the correlation between PM_{2.5} and O₃ compared to meteorological conditions.

3.2. Comparison of O₃ Variations at Different Sites in India

Table 1 shows the daytime average maximum concentrations of O₃ over different locations in India. From the table, it is highlighted that the highest levels of O₃ are detected during the winter and summer months in the south-western areas of India. The increased O₃ levels in winter are primarily attributed to local emissions of precursor gases, the transportation of pollutants from distant areas, and the existence of a shallow Atmospheric Boundary Layer (ABL) height. In all regions, the levels of O₃ decrease significantly during the monsoon season as a result of reduced photochemical reactions caused by heavy rainfall, insufficient solar radiation, and the strong marine influence.

Table 1. Observed daytime average/maximum surface O₃ concentrations over different locations in India.

Locations	Category	Daytime Average/Maximum (ppbv) (Season)	Reference
Doon Valley	Himalaya region	63.8 ± 15.3 (Pre monsoon)	[69]
Ahmedabad	Semi-arid urban	40–60 (Summer)	[70]
Aizwal	Himalayan Valley	27.1 (Pre-Monsoon)	[73]
Tezpur	Himalayan Valley	31.0 (Pre-Monsoon)	[73]
Guwahati	River valley	18.31 ± 5.8 Pre monsoon	[75]
Hyderabad	Sub-urban region	35.54 ± 7.16 (Winter)	[76]
Jodhpur	Semi-arid,	47 ± 11.5 (Pre monsoon)	[79]
Agra	Urban	32.5 ± 19.3 (Summer)	[81]
Udaipur	Semi-arid	46 ± 12.5 (Pre monsoon)	[82]
NCR Delhi	Urban	45.3 ± 9.5 (Winter)	[84]
Port Blair	Marine site	30 ± 5 (Winter)	[86]
Pantnagar	Semi-Urban	48.7 ± 13.8 (Spring)	[89]
Bhubaneswar	Urban	61.7 ± 12.7 (Winter)	[90]
Dibrugarh	Sub Himalayan	42.9 ± 10.3 (Pre monsoon)	[91]
Kanpur	Urban	27.9 ± 17.8 (Summer)	[92]
Dayalbag	Suburban	56 ± 10.8 (Summer)	[95]

Table 1. Cont.

Locations	Category	Daytime Average/Maximum (ppbv) (Season)	Reference
Kannur Town	Urban city	48.25 ± 7.2 (Winter)	[104]
Kannur University	Rural	35.47 ± 10.5 (Winter)	[105]
Trivandrum	Coastal	40 ± 8.5 (Winter)	[106]
Anantapur	Semi-arid, Rural	64.9 ± 5.3 (Summer)	[107]
Ootty	High altitude	53.5 ± 8.2 (Winter)	[108]

During the winter season, Kannur, Trivandrum, Delhi, Port Blair, Bhubaneswar, Ooty, and Hyderabad experience the most elevated levels of O₃ concentrations. Conversely, Agra, Kanpur, the Indo-Gangetic Plain, Dayalbagh, and Anantapur showcase extreme levels of O₃ concentrations in the summer season. During the pre-monsoon season, elevated levels of O₃ are detected in the northern and north-eastern regions of India. The increase in O₃ levels observed during night-time hours in the mountainous areas of the Himalayan valley can be attributed to the intrusion of O₃ from the free troposphere. The formation and chemistry of surface O₃ are predominantly impacted by the marine environment in the south Indian sites as a result of their close proximity to oceans. Conversely, surface O₃ production in northern Indian areas is primarily influenced by the land environment, while the mountainous regions in the northeast have a significant impact on this process. Thus, the variations in surface O₃ levels across different locations in the Indian subcontinent are primarily influenced by changes in latitude/longitude, meteorological shifts, solar radiation intensity, atmospheric boundary layer height, precursor gas levels, and human activities, as determined by O₃ chemistry and transport analysis.

4. Surface O₃ Measurements in the Kerala Region

Kerala, located in the southern region of India, is a state that extends along the coastline of the Arabian Sea. The state is heavily impacted by the marine surroundings and is currently confronting a notable problem of air pollution caused by the rising emissions from vehicles and development activities. Even though Kerala lacks a large number of industries, it is struggling with this escalating concern of air pollution. There are only a few institutions and organizations in Kerala actively engaged in studying the levels of surface O₃ through ground-based observations to assess the atmospheric chemistry and transport of trace gases. The southwest monsoon begins in Kerala during the initial week of June, introducing marine influences throughout spring and summer whereas during winter and autumn, the atmosphere is affected by the landmass. This significant disparity in marine influence leads to an intricate atmospheric chemistry and the movement of air pollutants.

Resmi [104] conducted a study aimed at characterizing the diurnal and seasonal fluctuations of O₃ and its precursors, including NO_x, CO, VOCs, and other trace gases, throughout the period of 2019–2020 in the urban setting of Kannur town, situated in the northern region of Kerala state. The study revealed that the seasonal distribution of pollutants exhibited peak concentrations during the winter months, attributed to long-distance transportation and heightened local emissions. Furthermore, a notable reduction in trace air pollutants, with the exception of O₃, was observed on weekends in comparison to weekdays, suggesting that the sources of these pollutants were predominantly linked to vehicular and industrial activities. Interestingly, the levels of O₃ displayed an increasing trend on weekends as opposed to weekdays, with a more pronounced percentage rise noted during the winter season than in summer. Moreover, based on the statistical analysis, it was suggested that Kannur Town is an area highly susceptible to volatile organic compounds (VOCs), which play a crucial role in regulating the photochemical generation of O₃ even in the presence of relatively low levels of NO_x. In another study, Resmi [105] examined the prolonged changes in surface O₃ and NO_x levels at Kannur University campus, situated in a rural area in north Kerala. Their findings indicated that various climatic elements, including solar

radiation, atmospheric temperature, and NO_2 concentrations have a substantial impact on the photochemical generation and depletion of surface O_3 . Through the implementation of an artificial neural network analysis, it was determined that atmospheric temperature has a positive correlation with O_3 production at the observation site. Furthermore, the study revealed a consistent enhancement in O_3 values from 2013 to 2018.

Nair [106] conducted a study on the long-term variations in surface O_3 levels. Their findings highlight a significant rise in O_3 concentration at Thiruvanthapuram in Kerala. The study revealed a 10 ppbv increase in O_3 concentration between 1973 and 2012, with the highest rate of increase occurring from 2005 to 2009 at a rate of 2 ppbv per year. Girach [109] conducted an investigation on the impact of the COVID-19 lockdown on surface O_3 and NO_2 levels at Thumba in Thiruvananthapuram. The findings revealed a notable decrease in the concentration of daytime surface O_3 and NO_2 , with reductions of 36% and 40%, respectively. Furthermore, an interesting observation was made during the onset of land breeze, where a rise in O_3 levels was detected. This rise had a magnitude ranging from 5 to 10 ppbv. In order to study this phenomenon, the researchers employed a photochemical box model. Through this model, it was determined that the transportation of O_3 -enriched air during the onset of land breeze played a significant role in the observed rise at Thumba. Variations in surface O_3 at the same location between 2007 and 2009 indicated that the daytime O_3 pattern was closely linked to mesoscale movements and the availability of NO_x [110].

The daytime rise in O_3 persists until the onset of land breeze. The elevated O_3 levels observed in winter are attributed to the presence of north-easterly winds that transport precursor gases to the study area. It was also revealed that one molecule of NO_x or NO_2 is responsible for generating approximately seven to nine molecules of O_3 at that specific site. A similar investigation by Nair [111] demonstrated varying diurnal O_3 patterns. They determined that the wind profile at Thumba significantly influenced the photochemical generation of O_3 . During night time, polluted air from the land side moves towards the adjacent oceanic region, moderately increasing the levels of O_3 and precursor gases.

The research conducted by Nishanth [112] at Mangattuparamba, Kannur University campus was centred on the surveillance of O_3 and NO_x levels through ground-based observations. The findings indicated that O_3 concentration reached its highest point in the late afternoon throughout the year mainly due to the heightened O_3 production resulting from the photolysis of NO_x . They also identified the presence of a vapour phase in the ambient air at this site, containing alkanes, alkenes, aldehydes, and organic acids. These compounds contributed to higher levels of volatile organic compounds (VOCs), thereby aiding in O_3 production through the VOC– NO_x cycle. Another study conducted by Nishanth [113] investigated the impact of precursor gases and particulate matter (PM) on the fluctuation of surface O_3 levels in Kannur. In the winter season, a notable relationship was discovered between O_3 and its precursor CH_4 . Additionally, a negative association between PM and surface O_3 indicated the influence of aerosols on O_3 generation in Kannur. The study also emphasized the substantial contribution of marine sources in Mangattuparamba. It was noted that the differences in O_3 and NO_x concentrations between weekdays and weekends were insignificant in Mangattuparamba, while these differences were more evident in Kannur Town, an urban area greatly affected by vehicular traffic.

Revathy [114] conducted an analysis on the variations in surface O_3 concentrations at Ponnudi, a high-altitude location situated in the southern region of the Western Ghats. The research revealed that reduced O_3 levels were associated with higher dry deposition loss and the biogenic release of isoprene across the Western Ghats. Also they found that regional pollution from the urban boundary layer and downdraft of rich air during night are mainly influencing the diurnal pattern of O_3 over Ponnudi.

5. Long-Term Variation in Surface O₃ over Two Locations in Kannur

The importance of surface O₃ and its precursors was acknowledged by the Indian Space Research Organisation (ISRO) through the establishment of Atmospheric Chemistry, Transport and Modelling (AT-CTM) networks of stations in 2008 as part of the Geosphere, Biosphere Program (GBP) across various regions of the Indian subcontinent. Following this, Kannur was designated as a key site on the west coast of India, leading to the establishment of an atmospheric observatory under ISRO-GBP in 2009. Figure 1 shows the boundary map of India, Kerala, and Kannur district.

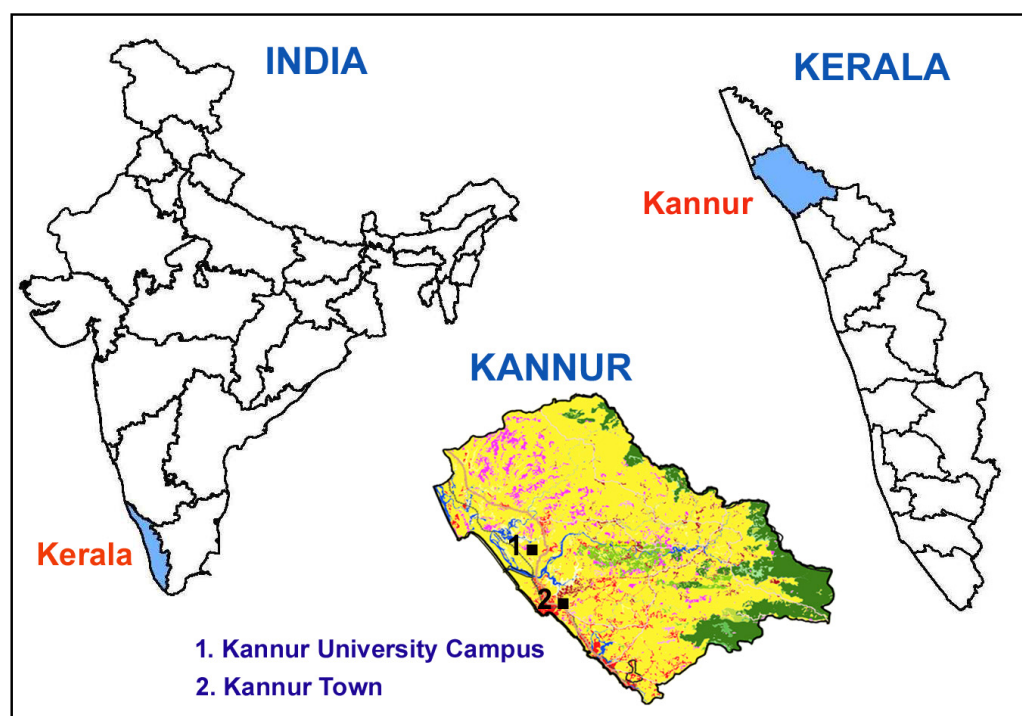


Figure 1. Map of India, Kerala, and Kannur district.

This segment focuses on the examination of surface O₃ fluctuations at a rural site (Kannur University Campus) and an urban site (Kannur Town) within the Kannur district of Kerala in South India. The measurements were taken at both a rural location (Kannur University Campus) and an urban location (Kannur Town). The annual average diurnal variations in surface O₃ at Kannur University Campus (during 2016–2020) and Kannur Town (during 2019–2023) are depicted in Figure 2. Both locations exhibit similar diurnal patterns in O₃ levels, but with varying amplitudes. In the rural area, O₃ reaches its peak concentration (41.59 ± 8.6 ppbv) in the afternoon (15:00 h) and its lowest (6.82 ± 1.45 ppbv) in the early morning (04:00 h). Conversely, in the urban area, O₃ peaks (34.12 ± 4.8 ppbv) in the afternoon (13:30 h) and hits its lowest point (9.82 ± 2.81 ppbv) in the early morning (04:30 h). During the day, ozone concentration is elevated in the rural area (17.96% greater than in the urban area), whereas at night, ozone levels are higher in the urban setting (30% more than in the rural area) as a result of the high pollution levels in the urban location.

These variances stem mainly from differences in the photochemical reaction of precursor gases. Resmi [104] observed a lower level of NO and NO₂ at the rural site compared to the urban site. Consequently, the titration of O₃ with NO decreases at the rural site, leading to a predominance of photochemical production over the photochemical loss of O₃. Therefore, O₃ concentration appears to rise during daytime hours at the rural site in comparison to the urban site.

It becomes clear that the diurnal changes of O₃ exhibited a similar pattern across all seasons, albeit with varying concentrations at the two sites. The highest concentration of O₃ was observed during the winter months, followed by summer and postmonsoon, while

the lowest concentration was recorded during the monsoon season. Over the observational sites, O_3 concentration starts to upsurge in tune with solar radiation from the morning hours and reaches its extreme level (30–58 ppbv) at noon time hours, and it tends to decline in the evening hours and reaches its lower level (6–15 ppbv) in the night hours. The strongest O_3 build up during winter seasons is mainly due to the intense photochemical reactions of precursor gases and the stronger vertical transport over Kannur [115]. In addition to a higher concentration of precursors, shallow ABL height, intense solar radiation, and very low precipitation during the winter season support a higher concentration of O_3 production.

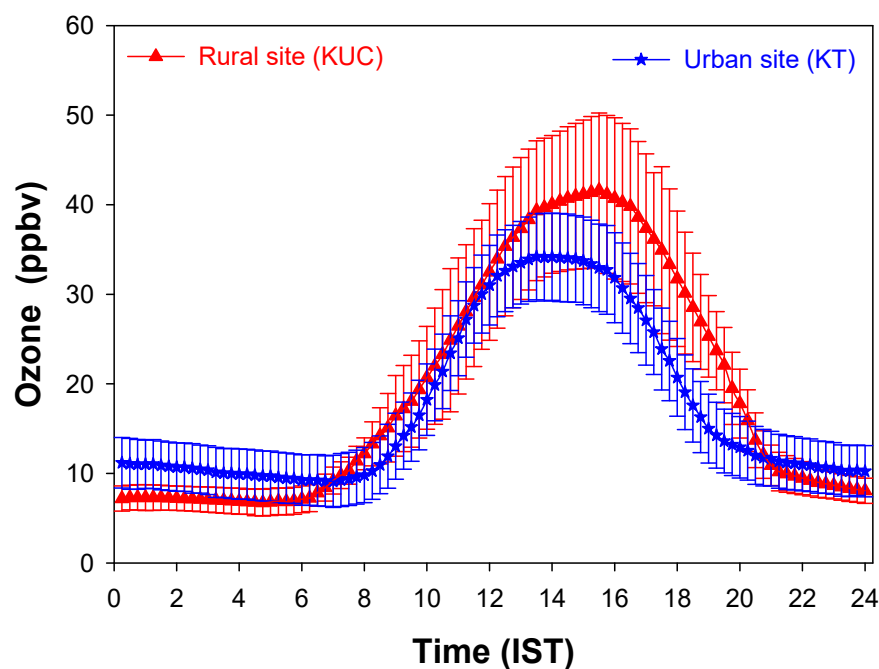


Figure 2. Annual average diurnal variation in surface O_3 over rural and urban location in Kannur.

At the rural site (Kannur University Campus), during the winter season, maximum (51.44 ± 5.2 ppbv) and minimum (7.45 ± 2.8 ppbv) levels of O_3 are observed at 13:30 h and at 05:00 h, and in summer, maximum (41.50 ± 5.5 ppbv) and minimum (6.42 ± 3.18 ppbv) concentrations are found at 14:00 h and at 06:00 h, respectively. During monsoon season, the maximum (20.62 ± 3.96 ppbv) levels are observed at 14:15 h, and in post-monsoon periods, the highest (29.51 ± 5.05 ppbv) concentrations are recorded at 14:00 h, respectively. At the urban site, during the winter season, maximum (45.24 ± 6.02 ppbv) and minimum (10.5 ± 2.15 ppbv) levels of O_3 are observed at 14:30 h and at 05:30 h, and in the summer, maximum (37.0 ± 6.4 ppbv) and minimum (9.42 ± 2.18 ppbv) concentrations are found at 14:30 h and at 06:00 h, respectively. During monsoon season, the maximum (19.24 ± 4.26 ppbv) levels are observed at 14:00 h, and in post-monsoon periods the highest (28.21 ± 5.75 ppbv) concentrations are recorded at 15:00 h, respectively. The rate of change in O_3 with respect to time, $[d(O_3)/dt]$ for various seasons over the rural and the urban location is shown in Figure 3.

During the winter season, the rate of change reaches its maximum in both locations due to the active photochemical reactions taking place within a shallow boundary layer. This rate is of the order of 9.4 ppbv h^{-1} and 10.4 ppbv h^{-1} at 10:00 h and 11:00 h at the rural site and 4.8 ppbv h^{-1} and 7.5 ppbv h^{-1} at 10:00 h and 11:00 h at the urban location, respectively. The rate of decrease is high during the evening and is in the order of 10.6 ppbv h^{-1} and 11.3 ppbv h^{-1} at 18:00 h and 19:00 h at the rural site and 8.5 ppbv h^{-1} and 9.2 ppbv h^{-1} at 18:00 h and 19:00 h at the urban location, respectively. The maximum $[d(O_3)/dt]$ in winter is 10.4 ppbv h^{-1} at 11:00 h at the rural location and 7.5 ppbv h^{-1} at 11:00 h at the urban location. The $[d(O_3)/dt]$ is almost zero at 14:00 h in the winter

and summer season for both the rural and urban location. During the midnight hours $[d(O_3)/dt]$ is found to be almost steady.

Urban areas experience slow rates of O_3 formation and a reduction in the morning and evening, while rural regions undergo rapid rates of O_3 generation and reduction during those periods. This difference can be primarily attributed to the lower levels of ambient air pollution found in rural locations. Additionally, regardless of whether it is a rural or urban setting, the rates of O_3 production and destruction are notably higher in the winter season compared to summer. This is due to the influence of land mass during winter and marine impact during summer. The presence of a shallow boundary layer in winter significantly impacts O_3 chemistry and its dispersion [89,116]. The severity of air pollution in a region is usually determined by assessing the O_3 production rate in the morning and its lapse rate in the late evening. Moreover, the comprehensive investigation reveals that the rapid decline in O_3 concentrations during winter evenings is markedly impacted by the ambient air pollution in comparison to the summer season. Consequently, a reduction in this decline indicates a shift from a pure environment to a polluted one, which can be evaluated by analysing the rate of O_3 modification. Similarly, the reduction in O_3 production at 14:00 h can be attributed to the influence of the sea breeze that impacts the rural area significantly during the winter season. This highlights the significant susceptibility of rural regions in the production of O_3 to sudden changes in atmospheric environment. The statistical analysis of the observed concentration of O_3 at the rural and urban site is listed in Table 2.

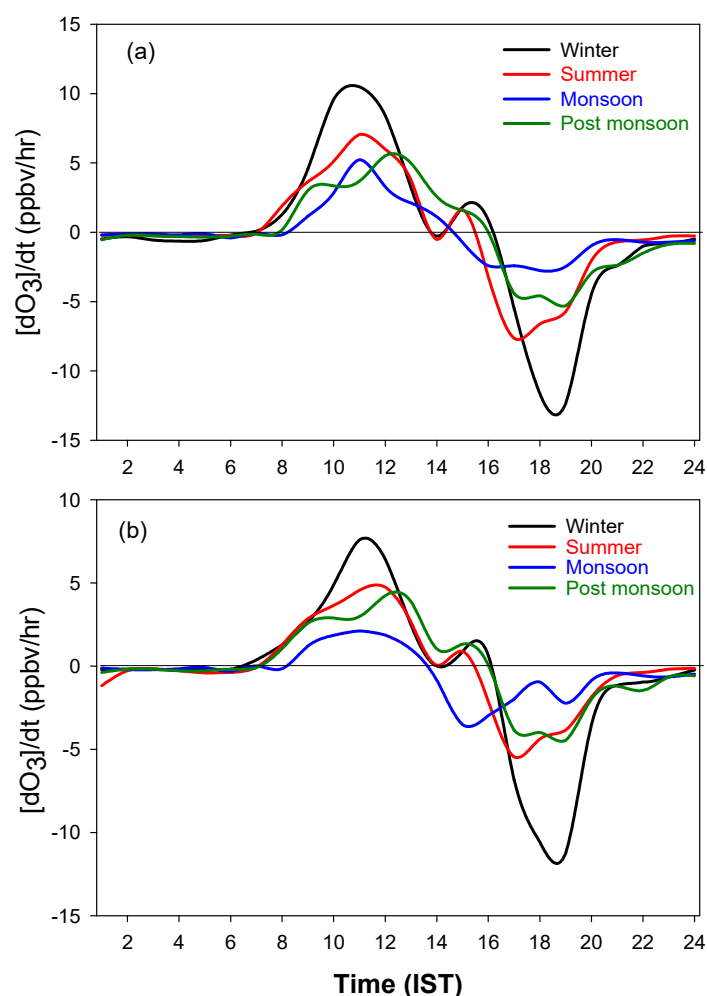


Figure 3. Seasonal variations in the rate of change in O_3 at (a) rural location (b) urban location.

Table 2. Statistical analysis of the observed O₃ levels at the rural and urban site.

Period of Observation at Rural Site	Statistics	O ₃ Concentration (ppbv)	Period of Observation at Urban Site	Statistics	O ₃ Concentration (ppbv)
1 January 2016– 31 December 2016	Average	34.38	1 January 2019– 31 December 2019	Average	34.38
	Standard deviation	11.1		Standard deviation	11.48
	Daytime maximum	56.12		Daytime maximum	46.78
	Daytime minimum	12.4		Daytime minimum	13.58
	Number of datapoints	41,760		Number of datapoints	36,540
1 January 2017– 31 December 2017	Average	35.12	1 January 2020– 31 December 2020	Average	32.33
	Standard deviation	12.2		Standard deviation	10.56
	Daytime maximum	57.6		Daytime maximum	48.52
	Daytime minimum	12.02		Daytime minimum	14.42
	Number of datapoints	40,880		Number of datapoints	37,560
1 January 2018– 31 December 2018	Average	35.47	1 January 2021– 31 December 2021	Average	32.78
	Standard deviation	10.5		Standard deviation	11.87
	Daytime maximum	58.5		Daytime maximum	47.98
	Daytime minimum	12.45		Daytime minimum	13.96
	Number of datapoints	39,320		Number of datapoints	38,440
1 January 2019– 31 December 2019	Average	35.97	1 January 2022– 31 December 2022	Average	33.32
	Standard deviation	8.52		Standard deviation	11.41
	Daytime maximum	59.21		Daytime maximum	48.98
	Daytime minimum	12.68		Daytime minimum	13.38
	Number of datapoints	36,558		Number of data points	37,960
1 January 2020– 31 December 2020	Average	36.42	1 January 2023– 31 December 2023	Average	33.88
	Standard deviation	9.6		Standard deviation	11.54
	Daytime maximum	59.85		Daytime maximum	50.21
	Daytime minimum	12.18		Daytime minimum	14.28
	Number of datapoints	40,240		Number of datapoints	38,540

During the period of January to December 2015, the rural site exhibited an average O₃ concentration of 33.75 ± 10.6 ppbv, which increased to 36.42 ± 9.6 ppbv in the same period in 2020. This indicates a 7.91% rise in O₃ levels over the six-year span from 2015 to 2020 at the rural site. In contrast, the urban site showed an average O₃ concentration of 32.14 ± 11.48 ppbv during January to December 2019, which increased to 33.88 ± 11.54 ppbv in the same period in 2020, reflecting a 5.41% increase. The investigation carried out by Resmi [104] unveiled the sensitivity O₃ production in the urban region of Kannur to volatile organic compounds (VOCs).

6. Surface O₃ Variations during Special Episodes in India

Surface O₃ formation and destruction is dependent on emissions, concentrations, and ratios of precursors and intensity of solar radiation. Fireworks and solar eclipses provide unique opportunities to conduct a detailed study of the short-term changes in the atmospheric chemistry of surface O₃. The following section describes the variation in surface O₃ during fireworks and solar eclipse episodes.

6.1. Surface O₃ Variations during Fireworks

Indian festivals and cultural events are deeply embedded in the social structure, showcasing the abundant diversity and heritage of the nation. However, the use of fireworks during these events poses significant challenges, especially in terms of air quality and public health. The captivating display of vibrant colours against the dark sky may attract a diverse audience, but it is essential to consider the potential consequences on atmospheric air and public well-being. Several research studies have highlighted the adverse effects of fireworks on air quality, particularly in densely populated regions where festivals are prevalent [117–120]. Burning fireworks leads to the release of various pollutants, such as particulate matter, sulphur compounds, and heavy metals, which can remain in the atmosphere and contribute to air pollution. The presence of surface O₃ pollution during fireworks is a major issue, especially in urban areas where celebrations are frequent. Although fireworks do not directly emit substantial amounts of O₃, they can contribute to its formation through chemical reactions involving NO₂ and VOCs in the atmosphere. A study by Attri [121] proposed a pathway for the creation of ground-level O₃ due to the combustion of fireworks.

Limited research has been conducted to investigate the impact of fireworks on surface O₃ levels in India. These studies typically involve monitoring O₃ concentrations before, during, and after fireworks events, as well as analysing the atmospheric chemical composition to understand the factors contributing to O₃ formation. Diwali, a festival of lights, widely celebrated in India, involves the widespread use of fireworks as a crucial part of the celebrations. Ganguly [122] conducted a study examining the changes in O₃ and various air pollutants in nine major cities in India during the Diwali festival in 2016. The study revealed a significant increase in the concentration of O₃ and other pollutants during the period when fireworks were set off.

Mandal [123] explored the differences in air pollution levels during Diwali celebrations amidst the COVID-19 pandemic in 2020 compared to the previous year. They observed that the level of major air pollutants including O₃ was substantially higher in 2020 than 2019 due to the usage of more firecrackers in 2020 than the preceding year. Saxena [124] analysed the atmospheric pollutants such as O₃, NO_x, and PM during the Diwali fireworks at a residential site in Delhi in 2016 and 2017, and found a sharp increase in the quantity of pollutants on the Diwali day due to the combustion of fireworks. Garg [125] conducted a study on the impact of firecracker detonation on air quality in Delhi over a six-year period from 2010 to 2015. The researchers found significant increases in O₃, PM, and NO₂ concentrations compared to the month before the festivities. Ambade [126] also investigated O₃ and other trace pollutants during the Diwali festival in Jamshedpur in 2017, revealing levels that exceeded the National Ambient Air Quality Standard (NAAQS).

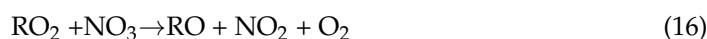
Additionally, Peshin [127] noted elevated levels of O₃, NO_x, and PM during Diwali in 2014, mainly due to firecracker burning.

Vishu is a major festival that is predominantly celebrated with night-time fireworks in the Indian state of Kerala on either April 14th or 15th, as per the Gregorian calendar. Resmi [128] has documented the changes in O₃ and other trace air pollutants levels during pre–post and Vishu days across two consecutive years (2020 and 2021) in Kannur town. The study found a 51% increase in O₃ concentration during the evening fireworks event on Vishu eve, along with a 61% rise during the early morning fireworks display on Vishu day. Furthermore, it was noted that the enforcement of COVID-19 lockdown measures in 2020 led to a decline in air pollution levels compared to previous years. Another examination conducted by the same researcher, Resmi [129], provides valuable insights into the air quality dynamics during the Vishu festival in Mangattuparamba, a rural area in Kannur. The research findings from the Vishu celebrations held between 2015 and 2018 clearly demonstrate a significant increase in O₃, PM, and NO₂ concentrations. This rise is directly linked to the emissions of pollutants released from fireworks, resulting in temporary spikes in air pollution. Both the model and observations confirm that the intensified photochemical production of NO₂ is the main factor contributing to the observed increase in O₃ levels during the fireworks displays in Mangattuparamba.

In 2010 and 2011, a study was carried out by Nishanth [130] on the night-time generation of O₃ during the Vishu festival fireworks. The results showed that the elevated levels of O₃ were directly linked to NO₂ photodissociation caused by the firecracker explosions. This resulted in a two-fold increase in O₃ concentration compared to normal days in both years. Using a UV–visible spectrophotometer, the researchers examined the emission spectra of the firecrackers and put forward a complex mechanism for O₃ production during the night-time fireworks show. Specifically, they proposed that the higher concentration of alkanes released into the gas phase during the fireworks primarily reacted with the OH radical to form alkyl radicals. These alkyl radicals then quickly combined with O₂ to generate alkyl peroxy (RO₂) radicals, following a reaction pathway suggested by Wilson [131].



RO₂ can further react with NO₃ radicals to form NO₂,



It was suggested that the peroxy radicals oxidise NO into NO₂, thus renewing OH. As a result, the NO₂ produced is photolyzed in the flash of firecrackers, producing O₃.

6.2. Surface O₃ Variations during Different Solar Eclipse

Solar eclipses offer a distinct opportunity for researchers to examine how different atmospheric parameters influence atmospheric dynamics across various regions of the world during the obscuration of sun for a short period of time. These celestial events lead to temporary alterations in solar insolation, temperature, and atmospheric circulation, ultimately impacting atmospheric chemistry, dynamics, and meteorological conditions [132–136]. Various studies were conducted focusing on the photochemistry of surface and stratospheric O₃ during solar eclipse episodes [137–141]. Manchanda [142] detected a notable decrease in O₃ levels in both the stratosphere and troposphere immediately following the peak of the eclipse in Thiruvananthapuram on 15 January 2010. This drop can be attributed to the decrease in temperature and solar actinic flux caused by the eclipse. Anoop [143] observed a gradual decline in surface O₃ concentrations during the eclipse event on 26 December 2019 in Kozhikode, a northern coastal city in Kerala. The decrease in O₃ levels was associated with the decrease in solar irradiance due to the eclipse and the decrease in NO₂ mixing ratios as a result of reduced convection. Jain [144] reported a 48% reduction in surface O₃

levels and an 8% increase in NO₂ levels, coinciding with a decrease in solar irradiance during the solar eclipse that occurred on 26th December 2019 in South India.

Resmi [145] explored the changes in surface and total column O₃ levels, as well as other trace air pollutants, during an annular solar eclipse that took place on 26 December 2019 in Kannur town, Kerala. The study revealed a significant decrease in surface O₃ concentration by 61.5% and total column O₃ by 11.8%, along with a 93% reduction in solar radiation at the peak of the solar eclipse. Model simulations were employed to elucidate the variations in photodissociation coefficient $j(\text{NO}_2)$ values, showing a strong agreement with the decrease in $j(\text{NO}_2)$ as simulated by the model. The investigation carried out by Nishanth [146] determined that the solar eclipse on 15 January 2010 had a significant impact on surface O₃ levels and meteorological parameters in Kannur. Solar radiation and O₃ levels decreased by 89% and 57.5%, respectively, while NO_x levels increased by 62.5% during the eclipse's peak. The decline in O₃ and NO_x levels was attributed to the decrease in NO₂ photolysis rates, as indicated by the model simulation. The model's simulated O₃ reduction of 59% closely aligned with the observed reduction of 57.5% during the eclipse.

Sharma [147] observed a decrease in surface O₃ and NO₂ levels after the start of a solar eclipse in Thiruvananthapuram on 15 January 2010. Their research indicated a notable drop in surface O₃ only 22 min into the eclipse's full phase. Additionally, they recorded a decline in ambient temperature and wind speed, as well as an uptick in relative humidity during the solar eclipse event. Akhil [148] carried out a study focusing on the fluctuations in O₃ vertical distribution during the solar eclipse that occurred on 26 December 2019 in Gadanki. The research involved the use of ozonesonde and multiple instruments. The results demonstrated a rise in upper tropospheric O₃ levels immediately after the solar eclipse, while a decline in total O₃ was noted during the peak of solar obscuration. By examining meteorological parameters, MST radar observations, and back trajectory simulations, it was concluded that the observed O₃ elevation was influenced by a stratospheric exchange pre-eclipse and long-distance transportation facilitated by the sub-tropical jet stream passing over Gadanki.

7. Conclusions

Surface O₃ is an air pollutant with oxidizing capacity, originating close to the Earth's surface through the interaction of its precursors under sunlight. It is a secondary air pollutant derived from primary pollutants such as NO_x and VOCs. The smog prevalent during the winter season in India and China is primarily caused by surface O₃. This analysis presents a historical summary of surface O₃ measurements carried out at network centres in India. Long-term O₃ monitoring stations throughout the country have shown that the production of surface O₃ is greatly influenced by factors such as geography, latitude, marine impact, and local air pollution. Additionally, there is a noticeable variation in the timing of peak O₃ concentrations. The highest levels of surface O₃ are mainly observed during the summer/pre-monsoon months in dry regions due to increased precursor gases. Conversely, during the winter months, the peak O₃ levels have been recorded in areas near mountainous regions in North India. On the other hand, O₃ levels peak during the winter months in southern regions of India due to clear skies and extensive long-range air mass transport. The elevated levels of precursors leading to surface O₃ in autumn and winter are a result of continent-wide transport and lower boundary layer heights. This analysis also seeks to highlight the current studies focusing on surface O₃ levels conducted across a network of environmental observatories in India, particularly in rural areas.

The review emphasized the difference in O₃ production rates between two distinct urban and rural locations in Kannur. The maximum production rate at the rural location is 10.4 ppbv h⁻¹ at 11.00 h, while the urban location has a production rate of 7.5 ppbv h⁻¹ at the same time. The Kannur university campus is considered a rural location, while Kannur town is an urban site located approximately 15kms away from the rural location. Additionally, both sites show an increasing trend in surface O₃, with a 7.91% increase in the rural location over five years from 2016 to 2020, and a 5.41% increase in the urban

location over five years from 2019 to 2023. This observation highlights a significant rise in O₃ production rate in the rural area of Kannur compared to its urban counterpart.

An abrupt change in the surface O₃ concentration is detected during unique events such as solar eclipses and fireworks. The data collected during these occurrences can lead to changes in the typical chemistry related to the generation and removal of trace gases. These specific events, each with their own characteristics, play a role in shaping the overall atmospheric chemistry of the location. The gradual decrease and subsequent rise in surface O₃ levels during the solar eclipse, along with its effects on meteorological factors, and the increase in surface O₃ levels at night during fireworks shows, pose a unique challenge for scientific investigation.

The assessment has been compiled by selecting the most relevant literature detailing the changes in surface O₃ caused by precursors and meteorological factors. Nevertheless, it is not exhaustive as we could not include additional research due to space limitations.

Author Contributions: Conceptualization, K.A.K.L., T.N. and M.K.S.K.; Methodology, M.K.S.K. and T.N.; software, T.N. and K.A.K.L.; validation, M.K.S.K. and K.T.V.; formal analysis, K.A.K.L., T.N., M.K.S.K. and K.T.V.; investigation, K.A.K.L., T.N. and M.K.S.K.; resources, T.N., M.K.S.K. and K.T.V.; data curation, T.N. and M.K.S.K.; writing—original draft preparation, K.A.K.L. and T.N.; writing—review and editing, T.N., M.K.S.K. and K.T.V.; supervision, T.N. and M.K.S.K.; project administration, T.N. and M.K.S.K.; funding acquisition, K.T.V. All authors have read and agreed to the published version of the manuscript.

Funding: This research received no external funding.

Institutional Review Board Statement: Ethical review and approval were not required for this study as it did not involve the use of humans or animals in the research process.

Informed Consent Statement: Informed consent was deemed unnecessary for this study since there were no human or animal subjects involved in the review process.

Data Availability Statement: This manuscript serves as a review, utilizing literature exclusively for the analysis without incorporating any data.

Acknowledgments: The authors wish to extend their sincere appreciation to the Indian Space Research Organisation (ISRO), Bangalore, for their invaluable support in the Atmospheric Chemistry, Transport, and Modeling (AT-CTM) project under the Geosphere Biosphere Programme. Furthermore, the authors are grateful to the Kerala State Pollution Control Board (KSPCB) for their assistance in researching air pollutants over Kerala region. Valsaraj acknowledges the generous support from the Charles and Hilda Roddey Distinguished Professorship at LSU. Authors express their thanks to Chinthu Viswanath, Sree Krishna College Guruvayur for his critical comments. Furthermore, the authors acknowledge their gratitude to four anonymous reviewers for their insightful feedbacks and critical comments to improve the manuscript in the present form.

Conflicts of Interest: The authors declare no conflict of interest.

References

1. Meo, S.A.; Salih, M.A.; Hussain, F.A.; Alkhalifah, J.M.; Meo, A.S.; Akram, A. Environmental pollutants PM_{2.5}, PM₁₀, carbon monoxide (CO), nitrogen dioxide (NO₂), sulfur dioxide (SO₂), and ozone (O₃) impair human cognitive functions. *Eur. Rev. Med. Pharmacol. Sci.* **2024**, *28*, 789–796. [[CrossRef](#)] [[PubMed](#)]
2. Masiol, M.; Hopke, P.K.; Felton, H.D.; Frank, B.P.; Rattigan, O.V.; Wurth, M.J.; LaDuke, G.H. Analysis of Major Air Pollutants and Submicron Particles in New York City and Long Island. *J. Atmos. Environ.* **2017**, *48*, 203–214. [[CrossRef](#)]
3. Mayer, H. Air pollution in cities. *J. Atmos. Environ.* **1999**, *33*, 4029–4037. [[CrossRef](#)]
4. Crutzen, P.J. The role of NO and NO₂ in the chemistry of the troposphere and stratosphere. *Annu. Rev. Earth Planet. Sci.* **1979**, *7*, 443–472. [[CrossRef](#)]
5. Prather, M.J.; Zhu, X.; Tang, Q.; Hsu, J.; Neu, J.L. An atmospheric chemist in search of the tropopause. *J. Geophys. Res.* **2011**, *116*, 2156–2202. [[CrossRef](#)]
6. Myhre, G.; Shindell, D.; Breion, F.-M.; Collins, W.; Fuglestedt, J.; Huang, J.; Koch, D.; Lamarque, J.-F.; Lee, D.; Mendoza, B.; et al. Anthropogenic and natural radiative forcing, in: Climate Change: The physical science basis. In *Contribution of Working Group I to the Fifth Assessment Report of the Intergovernmental Panel on Climate Change*; Cambridge University Press: Cambridge, UK; New York, NY, USA, 2013; pp. 659–740.

7. Staehelin, J.; Harris, N.R.P.; Appenzeller, C.; Eberhard, J. Ozone trends: A review. *Rev. Geophys.* **2001**, *39*, 231–290. [[CrossRef](#)]
8. Ramanathan, V.; Dickinson, R.E.J. The role of stratospheric O₃ in the zonal and seasonal radiative energy balance of the Earth-troposphere system. *Atmos. Sci.* **1979**, *36*, 1084–1104.
9. Archibald, A.T.; Neu, J.L.; Elshorbany, Y.; Cooper, O.R.; Young, P.J.; Akiyoshi, H.; Cox, R.A.; Coyle, M.; Derwent, R.; Deushi, M.; et al. Tropospheric ozone assessment report: A critical review of changes in the tropospheric ozone burden and budget from 1850 to 2100. *Elem. Sci. Anthr.* **2020**, *8*, 034. [[CrossRef](#)]
10. Tarasick, D.; Galbally, I.E.; Cooper, O.R.; Schultz, M.G.; Ancellet, G.; Leblanc, T.; Wallington, T.J.; Ziemke, J.; Liu, X.; Steinbacher, M.; et al. Tropospheric Ozone Assessment Report: Tropospheric ozone from 1877 to 2016, observed levels, trends and uncertainties. *Elem. Sci. Anthr.* **2019**, *7*, 39. [[CrossRef](#)]
11. Mills, G.; Pleijel, H.; Malley, C.S.; Sinha, B.; Cooper, O.R.; Schultz, M.G.; Neufeld, H.S.; Simpson, D.; Sharps, K.; Feng, Z.; et al. Tropospheric Ozone Assessment Report: Present-day tropospheric ozone distribution and trends relevant to vegetation. *Elem. Sci. Anthr.* **2018**, *6*, 47. [[CrossRef](#)]
12. Lefohn, A.S.; Malley, C.S.; Smith, L.; Wells, B.; Simon, H.; Naik, V.; Mills, G.; Schultz, M.G.; De Marco, A.; Xu, X.; et al. Tropospheric ozone assessment report: Global ozone metrics for climate change, human health, and crop/ecosystem research. *Elem. Sci. Anthr.* **2018**, *6*, 27. [[CrossRef](#)]
13. Fleming, Z.; Doherty, R.M.; Schneidmesser, E.; Malley, C.S.; Cooper, O.R.; Pinto, J.P.; Colette, A.; Xu, X.; Simpson, D.; Schultz, M.G.; et al. Tropospheric Ozone Assessment Report: Present-day ozone distribution and trends relevant to human health. *Elem. Sci. Anthr.* **2018**, *6*, 12. [[CrossRef](#)]
14. Gaudel, A.; Cooper, O.R.; Ancellet, G.; Barret, B.; Boynard, A.; Burrows, J.P.; Clerbaux, C.; Cuesta, J.; Cuevas, E.; Doniki, S.; et al. Tropospheric Ozone Assessment Report: Present-day distribution and trends of tropospheric ozone relevant to climate and global atmospheric chemistry model evaluation. *Elem. Sci. Anthr.* **2018**, *6*, 39. [[CrossRef](#)]
15. Gaudel, A.; Bourgeois, I.; Li, M.; Chang, K.-L.; Ziemke, J.; Sauvage, B.; Stauffer, R.M.; Thompson, A.M.; Kollonige, D.E.; Smith, N.; et al. Tropical tropospheric ozone distribution and trends from in situ and satellite data. *EGUsphere* **2024**, 1–51. [[CrossRef](#)]
16. Chameides, W.; Walker, J.C.G. A photochemical theory of tropospheric ozone. *J. Geophys. Res.* **1973**, *78*, 8751–8760. [[CrossRef](#)]
17. Camalier, L.; Cox, W.; Dolwick, P. The effects of meteorology on ozone in urban areas and their use in assessing O₃ trends. *J. Atmos. Environ.* **2017**, *41*, 7127–7137. [[CrossRef](#)]
18. Fiore, A.M.; Jacob, D.J.; Logan, J.A.; Yin, J.H. Long-term trends in ground level ozone over the contiguous United States, 1980–1995. *J. Geophys. Res. Atmos.* **1998**, *103*, 1471–1480. [[CrossRef](#)]
19. USEPA. *EPA's Report on the Environment 2008*, EPA/600/R-07/045F; USEPA: Washington, DC, USA, 2008; p. 20460.
20. Solomon, P.; Cowling, E.; Hidy, G.; Furiness, C. Comparison of scientific findings from major ozone field studies in North America and Europe. *Atmos Environ.* **2000**, *34*, 1885–1920. [[CrossRef](#)]
21. Bloomfield, P.; Royle, J.A.; Steinberg, L.J.; Yang, Q. Accounting for meteorological effects in measuring urban ozone levels and trends. *Atmos. Environ.* **1996**, *30*, 3067–3077. [[CrossRef](#)]
22. Cox, W.M.; Chu, S.H. Assessment of interannual ozone variation in urban areas from a climatological perspective. *Atmos. Environ.* **1996**, *30*, 2615–2625. [[CrossRef](#)]
23. Mickley, L.J.; Murti, P.P.; Jacob, D.J.; Logan, J.A.; Koch, D.M.; Rind, D. Radiative Forcing from Tropospheric Ozone Calculated with a Unified Chemistry-Climate Model. *J. Geophys. Res.* **1999**, *104*, 30153–30172. [[CrossRef](#)]
24. Patil, S.D.; Thompson, B.; Revadekar, J.V. On the variation of the tropospheric ozone over Indian region in relation to the meteorological parameters. *Int. J. Remote Sens.* **2009**, *30*, 2813–2826. [[CrossRef](#)]
25. Zerefos, C.; Kourtidis, K.A.; Melas, D.; Balis, D.; Zanis, P.; Katsaros, L.; Mantis, H.T.; Repapis, C.; Isaksen, I.; Sundet, J.; et al. Photochemical Activity and Solar Ultraviolet Radiation Modulation Factors (PAUR): An overview of the project. *J. Geophys. Res.* **2002**, *107*, D18. [[CrossRef](#)]
26. Alvarez, R.; Weilenmann, M.; Favez, J.Y. Evidence of increased mass fraction of NO₂ within real world NO_x emissions of modern light vehicles derived from a reliable online measuring method. *Atmos. Environ.* **2008**, *42*, 4699–4707. [[CrossRef](#)]
27. Aneja, V.P.; Businger, S.; Li, Z.; Ciaiborn, C.S.; Murthy, A. Ozone climatology at high elevations in the southern Appalachians. *J. Geophys. Res.* **1991**, *96*, 1007–1021. [[CrossRef](#)]
28. Bonasoni, P.; Laj, P.; Angelini, F.; Arduini, J.; Bonafè, U.; Calzolari, F.; Cristofanelli, P.; Decesari, S. The ABC-Pyramid Atmospheric Research Observatory in Himalaya for aerosol, O₃ and halocarbon measurements. *Sci. Total Environ.* **2008**, *391*, 252–261. [[CrossRef](#)] [[PubMed](#)]
29. Bossioli, E.; Tombrou, M.; Dandou, A.; Soulakellis, N. Simulation of the effects of critical factors on ozone formation and accumulation in the greater Athens area. *J. Geophys. Res.* **2007**, *112*, D02309. [[CrossRef](#)]
30. Burley, J.D.; Bytnerowicz, A.; Ray, J.D.; Schilling, S.; Allen, E.B. Surface ozone in Joshua tree national park. *J. Atmos. Environ.* **2014**, *87*, 95–107. [[CrossRef](#)]
31. Chandra, N.; Venkataramani, S.; Lal, S.; Pozzer, A. Effects of convection and long-range transport on the distribution of carbon monoxide in the troposphere over India. *Atmos. Pollut. Res.* **2016**, *7*, 775–785. [[CrossRef](#)]
32. Feng, T.; Zhao, S.; Zhang, X.; Wang, Q.; Liu, L.; Li, G.; Tie, X. Increasing wintertime ozone levels and secondary aerosol formation in the Guanzhong basin, central China. *Sci. Total Environ.* **2020**, *745*, 140961. [[CrossRef](#)] [[PubMed](#)]
33. Finch, D.P.; Palmer, P.I. Increasing ambient surface ozone levels over the UK accompanied by fewer extreme events. *J. Atmos. Environ.* **2020**, *237*, 117627. [[CrossRef](#)]

34. Han, S.; Zhang, M.; Zhao, C.; Lu, X.; Ran, L.; Han, M.; Li, P.; Li, X. Differences in ozone photochemical characteristics between the megacity Tianjin and its rural surroundings. *J. Atmos. Environ.* **2013**, *79*, 209–216. [[CrossRef](#)]
35. Jung, H.C.; Moon, B.K.; Wie, J. Seasonal changes in surface ozone over South Korea. *Heliyon* **2018**, *4*, e00515. [[CrossRef](#)] [[PubMed](#)]
36. Kourtidis, K.; Zerefos, C.; Rapsomanikis, S.; Simeonov, V.; Balis, D.; Perros, P.E. Regional levels of O₃ in the troposphere over eastern Mediterranean. *J. Geophys. Res.* **2002**, *107*, 8140. [[CrossRef](#)]
37. Kunchala, R.K.; Singh, B.B.; Karumuri, R.K.; Attada, R.; Seelanki, V.; Kumar, N.K. Understanding the spatiotemporal variability and trends of surface ozone over India. *Environ. Sci. Pollut. Res. Int.* **2022**, *29*, 6219–6236. [[CrossRef](#)] [[PubMed](#)]
38. Mazzeo, A.N.; Venegas, E.L.; Choren, H. Analysis of NO, NO₂, O₃ and NO_x concentrations measured at a green area of Buenos Aires City during wintertime. *J. Atmos. Environ.* **2005**, *39*, 3055–3068. [[CrossRef](#)]
39. Moore, G.W.K.; Semple, J.L. High concentration of surface O₃ observed along the Khumbu Valley Nepal April 2007. *Geophys. Res. Lett.* **2009**, *36*, L14809. [[CrossRef](#)]
40. Qin, Y.; Tonnesen, G.S.; Wang, Z. One-hour and eight-hour average O₃ in the California south coast air quality management district: Trends in peak values and sensitivity to precursors. *Atmos. Environ.* **2004**, *38*, 2197–2207. [[CrossRef](#)]
41. Sanchez, M.L.; Garcia, M.A.; Pérez, I.A.; de Torre, B. Evaluation of surface ozone measurements during 2000–2005 at a rural area in the upper Spanish plateau. *J. Atmos. Chem.* **2018**, *60*, 137–152. [[CrossRef](#)]
42. Shan, W.; Yin, Y.; Zhang, J.; Ding, Y. Observational study of surface O₃ at an urban site in East China. *Atmos. Res.* **2008**, *89*, 252–261. [[CrossRef](#)]
43. Solberg, S.; Hov, Ø.; Søvde, A.; Isaksen, I.S.A.; Coddeville, P.; De Backer, H.; Forster, C.; Orsolini, Y.; Uhse, K. European surface O₃ in the extreme summer 2003. *J. Geophys. Res.* **2008**, *113*, D07307. [[CrossRef](#)]
44. Song, F.; Shin, J.Y.; Atresino, R.J.; Gao, Y. Relationships among the springtime ground-level NO_x, O₃ and NO₃ in the vicinity of highways in the US East Coast. *Atmos. Pollut. Res.* **2011**, *2*, 374–383. [[CrossRef](#)]
45. Strode, S.A.; Ziemke, J.R.; Oman, L.D.; Lamsal, L.N.; Olsen, M.A.; Liu, J. Global changes in the diurnal cycle of surface ozone. *Atmos. Environ.* **2019**, *199*, 323–333. [[CrossRef](#)]
46. Sun, Y.; Zhou, X.; Wai, K.; Yuan, Q.; Xu, Z.; Zhou, S.; Qi, Q.; Wang, W. Simultaneous measurement of particulate and gaseous pollutants in an urban city in North China Plain during the heating period: Implication of source contribution. *Atmos. Res.* **2013**, *134*, 24–34. [[CrossRef](#)]
47. Wallace, H.W.; Jobson, B.T.; Erickson, M.H.; McCoskey, J.K.; VanReken, T.M.; Lamb, B.K.; Vaughan, J.K.; Hardy, R.J.; Cole, J.L.; Strachan, S.M.; et al. Comparison of wintertime CO to NO_x ratios to MOVES and MOBILE6.2 on-road emissions inventories. *Atmos. Environ.* **2012**, *63*, 289–297. [[CrossRef](#)]
48. Yarwood, N.G.; Grant, J.; Koo, B.; Dunker, A.M. Modeling weekday to weekend changes in emissions and O₃ in the Los Angeles basin for 1997 and 2010. *Atmos Environ.* **2008**, *42*, 3765–3779. [[CrossRef](#)]
49. Naja, M.; Lal, S. Changes in surface ozone amount and its diurnal and seasonal patterns, from 1954–1955 to 1991–1993, measured at Ahmedabad (23°N). India. *Geophys. Res. Lett.* **1996**, *23*, 81–84. [[CrossRef](#)]
50. Fadnavis, S.; Anoop, S.M.; Choudhary, A.D.; Roy, C.; Singh, M.; Biswas, M.S.; Pandithurai, G.; Prabhakaran, T.; Lal, S.; Venkatraman, C.; et al. *Atmospheric Aerosols and Trace Gases: Assessment of Climate Change over the Indian Region*; Springer: Singapore, 2020. [[CrossRef](#)]
51. Henschel, S.; Querol, X.; Atkinson, R.; Pandolfi, M.; Zeka, A.; Tertre, A.; Analitis, A.; Katsouyanni, K.; Chanel, O.; Pascal, M.; et al. Ambient air SO₂ patterns in 6 European cities. *J. Atmos. Environ.* **2013**, *79*, 236–247. [[CrossRef](#)]
52. Wang, T.; Wei, X.L.; Ding, A.J.; Poon, C.N.; Lam, K.S.; Li, Y.S.; Chan, L.Y.; Anson, M. Increasing surface ozone concentrations in the background atmosphere of Southern China, 1994–2007. *Atmos. Chem. Phys.* **2009**, *9*, 6217–6227. [[CrossRef](#)]
53. Tsutsumi, Y.; Zaizen, T.; Makino, Y. Tropospheric ozone measurement at the top of Mt. Fuji. *Geophys. Res. Lett.* **1994**, *21*, 1727–1730. [[CrossRef](#)]
54. Oltmans, S.J. Long-term changes in tropospheric ozone. *Atmos. Environ.* **2006**, *40*, 3156–3173. [[CrossRef](#)]
55. Gupta, P.; Payra, S.; Bhatla, R.; Verm, S. WRF-Chem modeling study of heat wave driven ozone over southeast region, India. *Environ. Pollut.* **2024**, *340*, 122744. [[CrossRef](#)] [[PubMed](#)]
56. Pyrgu, A.; Hadjinicolaou, P.; Santamouris, M. Enhanced near-surface ozone under heatwave conditions in a Mediterranean island. *Nat. Sci. Rep.* **2018**, *8*, 9191. [[CrossRef](#)] [[PubMed](#)]
57. Zittis, G.; Hadjinicolaou, P.; Fnaiss, M. Projected changes in heat wave characteristics in the eastern Mediterranean and the Middle East. *Reg. Environ. Change* **2016**, *16*, 1863–1876. [[CrossRef](#)]
58. Zhang, G.; Xu, H.; Qi, B.; Du, R.; Gui, K.; Wang, H.; Jiang, W.; Liang, L.; Xu, W. Characterization of atmospheric trace gases and particulate matter in Hangzhou, China. *Atmos. Chem. Phys.* **2018**, *18*, 1705–1728. [[CrossRef](#)]
59. Monks, P.S.; Archibald, A.T.; Colette, A.; Cooper, O.; Coyle, M.; Derwent, R.; Fowler, D.; Granier, C.; Law, K.S.; Mills, G.; et al. Tropospheric ozone and its precursors from the urban to the global scale from air quality to short-lived climate forcer. *Atmos. Chem. Phys.* **2015**, *15*, 8889–8973. [[CrossRef](#)]
60. Seinfeld, J.H.; Pandis, S.N. *Atmospheric Chemistry and Physics from Air Pollution to Climate Change*; John Wiley and Sons: New York, NY, USA, 2006.
61. Carbon Brief Clear on Climate. Carbon Brief Profile, India. 2019. Available online: <https://www.carbonbrief.org/the-carbon-brief-profile-india> (accessed on 14 March 2019).

62. David, L.M.; Ravishankara, A.R. Boundary layer ozone across the Indian subcontinent: Who influences whom? *J. Geophys. Res. Lett.* **2019**, *46*, 10008–10014. [[CrossRef](#)]
63. Jethva, H.; Satheesh, S.K.; Srinivasan, J. Seasonal variability of aerosols over the Indo-Gangetic basin. *J. Geophys. Res.* **2005**, *110*, 1–15. [[CrossRef](#)]
64. Ojha, N.; Sharma, A.; Kumar, M.; Girach, I.; Ansari, T.U.; Sharma, S.K.; Singh, N.; Pozzer, A.; Gunthe, S.S. On the widespread enhancement in fine particulate matter across the Indo-Gangetic Plain towards winter. *Sci. Rep.* **2020**, *10*, 5862. [[CrossRef](#)]
65. Sinha, V.; Kumar, V.; Sarkar, C. Chemical composition of pre-monsoon air in the Indo-Gangetic Plain measured using a new air quality facility and PTR-MS: High surface ozone and strong influence of biomass burning. *Atmos. Chem. Phys.* **2014**, *14*, 5921–5941. [[CrossRef](#)]
66. Tripathi, N.; Sahu, L.K.; Wang, L.; Vats, P.; Soni, M.; Kumar, P.; Satish, R.V.; Bhattu, D.; Sahu, R.; Patel, K.; et al. Characteristics of VOC composition at urban and suburban sites of New Delhi, India in winter. *J. Geophys. Res. Atmos.* **2022**, *127*, e2021JD035342. [[CrossRef](#)]
67. Kumar, R.; Naja, M.; Venkataramani, S.; Wild, O. Variations in surface ozone at Nainital: A high-altitude site in the central Himalayas. *J. Geophys. Res.* **2010**, *115*, 1–12. [[CrossRef](#)]
68. Sarangi, T.; Naja, M.; Ojha, N.; Kumar, R.; Lal, S.; Venkataramani, S.; Kumar, A.; Sagar, R.; Chandola, H.C. First simultaneous measurements of ozone, CO, and NO_y at a high-altitude regional representative site in the central Himalayas. *J. Geophys. Res. Atmos.* **2014**, *119*, 1592–1611. [[CrossRef](#)]
69. Harithasree, S.; Sharma, K.; Girach, I.A.; Sahu, L.K.; Nair, P.R.; Singh, N.; Flemming, J.; Babu, S.S.; Ojha, N. Surface ozone over Doon valley of the Indian Himalaya: Characteristics, impact assessment, and model results. *J. Atmos. Environ. X* **2024**, *21*, 100247. [[CrossRef](#)]
70. Soni, M.; Ojha, N.; Imran, G. Impact of COVID-19 Lockdown on Surface Ozone Build-up at an Urban Site in Western India Based On Photochemical Box Modelling. *Curr. Sci.* **2021**, *120*, 376–381. [[CrossRef](#)]
71. Kumar, V.; Sinha, V. Season-wise analyses of VOCs, hydroxyl radicals and ozone formation chemistry over north-west India reveal isoprene and acetaldehyde as the most potent ozone precursors throughout the year. *Chemosphere* **2021**, *283*, 131184. [[CrossRef](#)]
72. Nelson, B.S.; Stewart, G.J.; Drysdale, W.S.; Newland, M.J.; Vaughan, A.R.; Dunmore, R.E.; Edwards, P.M.; Lewis, A.C.; Hamilton, J.F.; Acton, W.J.; et al. In situ ozone production is highly sensitive to volatile organic compounds in Delhi, India. *Atmos. Chem. Phys.* **2021**, *21*, 13609–13630. [[CrossRef](#)]
73. Tyagi, B.; Singh, J.; Beig, G. Seasonal progression of surface ozone and NO_x concentrations over three tropical stations in North-East India. *Environ. Pollut.* **2020**, *258*, 113662. [[CrossRef](#)]
74. Hama, S.M.L.; Kumar, P.; Harrison, R.M.; Bloss, W.J.; Khare, M.; Mishra, S.; Namdeo, A.; Sokhi, R.; Goodman, P.; Sharma, C. Four-year assessment of ambient particulate matter and trace gases in the Delhi-NCR region of India. *Sustain. Cities Soc.* **2020**, *54*, 102003. [[CrossRef](#)]
75. Dumka, U.C.; Gautam, A.S.; Tiwari, S.; Mahar, D.S.; Attri, S.D.; Chakrabarty, R.K.; Permita, P.; Hopke, P.K. Evaluation of urban O₃ in the Brahmaputra river valley. *Atmos. Pollut. Res.* **2020**, *11*, 610–618. [[CrossRef](#)]
76. Kanchana, A.L.; Sagar, V.K.; Pathakoti, M.; Mahalakshmi, D.V.; Mallikarjun, K.; Gharai, B. Ozone variability: Influence by its precursors and meteorological parameters- an investigation. *J. Atmos. Solar-Terr. Phys.* **2020**, *211*, 105468. [[CrossRef](#)]
77. Yadav, R.; Sahu, L.K.; Beig, G.; Tripathi, N.; Maji, S.; Jaaffrey, S.N.A. The role of local meteorology on ambient particulate and gaseous species at an urban site of western India. *Urban Clim.* **2019**, *28*, 100449. [[CrossRef](#)]
78. Bhardwaj, P.; Naja, M.; Rupakheti, M.; Lupascu, A.; Mues, A.; Panday, A.K.; Kumar, R.; Mahata, K.S.; Lal, S.; Lawrence, M.G. Variations in surface O₃ and CO in the Kathmandu Valley and surrounding broader regions during SusKat-ABC field campaign: Role of local and regional sources. *J. Atmos. Chem. Phys.* **2018**, *18*, 11949–11971. [[CrossRef](#)]
79. Pancholi, P.; Kumar, A.; Bikundia, D.S.; Chourasiya, S. An observation of seasonal and diurnal behavior of O₃-NO_x relationships and local/regional oxidant (OX = O₃ + NO₂) levels at a semi-arid urban site of western India. *Sustain. Environ. Res.* **2018**, *28*, 79–89. [[CrossRef](#)]
80. Mahapatra, P.S.; Kumar, R.; Mallik, C.; Panda, S.; Sahu, S.C.; Das, T. Investigation of a regional ozonereduction event over eastern India by integrating in situ and satellite measurements with WRF-Chem simulations. *Theor. Appl. Climatol.* **2018**, *137*, 399–416. [[CrossRef](#)]
81. Saini, R.; Taneja, A.; Singh, P. Surface ozone scenario and air quality in the north-central part of India. *J. Environ. Sci.* **2017**, *59*, 72–79. [[CrossRef](#)]
82. Yadav, R.; Sahu, L.K.; Beig, G.; Jaaffrey, S.N.A. Role of long-range transport and local meteorology in seasonal variation of surface ozone and its precursors at an urban site of India. *Atmos. Res.* **2016**, *176*, 96–107. [[CrossRef](#)]
83. Sharma, A.; Sharma, S.K.; Rohtash; Mandal, T.K. Influence of ozone precursors and particulate matter on the variation of surface ozone at an urban site of Delhi, India. *Sustain. Environ. Res.* **2016**, *26*, 76–83. [[CrossRef](#)]
84. Tyagi, S.; Tiwari, S.; Mishra, A.; Hopke, P.K.; Bisht, D.S. Spatial variability of concentrations of gaseous pollutants across the National Capital Region of Delhi, India. *Atmos. Pollut. Res.* **2016**, *7*, 808–816. [[CrossRef](#)]
85. Mallik, C.; Lal, S.; Venkataramani, S. Trace gases at a semi-arid urban site in western India: Variability and inter-correlations. *J. Atmos. Chem.* **2015**, *72*, 143–164. [[CrossRef](#)]

86. Mandal, T.K.; Peshin, S.K.; Sharma, C.; Raj, R.; Sharma, S.K. Study of surface ozone at Port Blair, India, a remote marine station in the Bay of Bengal. *J. Atmos. Solar Terr. Phys.* **2015**, *129*, 142–152. [[CrossRef](#)]
87. Lal, S.; Venkataramani, S.; Chandra, N.; Cooper, O.R.; Naja, M. Transport effects on the vertical distribution of tropospheric ozone over western India. *J. Geophys. Res.* **2014**, *119*, 10012–10026. [[CrossRef](#)]
88. Ojha, N.; Naja, M.; Sarangi, T.; Kumar, R.; Bhardwaj, P.; Lal, S.; Venkataramani, S.; Sagar, R.; Kumar, A.; Chandola, H.C. On the processes influencing the vertical distribution of ozone over the central Himalayas: Analysis of yearlong ozonesonde observations. *J. Atmos. Environ.* **2014**, *88*, 201–211. [[CrossRef](#)]
89. Ojha, N.; Naja, M.; Singh, K.P.; Sarangi, T.; Kumar, R.; Lal, S.; Lawrence, M.G.; Butler, T.M. Variabilities in O₃ at a semi-urban site in the Indo-Gangetic Plain region: Association with the meteorology and regional processes. *J. Geophys. Res.* **2012**, *117*, D20301. [[CrossRef](#)]
90. Mahapatra, P.S.; Panda, S.; Walvekar, P.P.; Kumar, R.; Das, T.; Gurjar, B.R. Seasonal trends meteorological impacts and associated health risks with atmospheric concentrations of gaseous pollutants at an Indian coastal city. *Environ. Sci. Pollut. Res.* **2014**, *21*, 11418–11432. [[CrossRef](#)] [[PubMed](#)]
91. Bhuyan, P.K.; Bharali, C.; Pathak, B.; Kalita, G. The role of precursor gases and meteorology on temporal evolution of O₃ at a tropical location in northeast India. *Environ. Sci. Pollut. Res.* **2014**, *21*, 6696–6713. [[CrossRef](#)] [[PubMed](#)]
92. Gaur, A.; Tripathi, S.N.; Kanawade, V.P.; Tare, V.; Shukla, S.P. Four-year measurements of trace gases (SO₂, NO_x, CO, and O₃) at an urban location, Kanpur, in Northern India. *J. Atmos. Chem.* **2014**, *71*, 283–301. [[CrossRef](#)]
93. Swamy, Y.V.; Venkanna, R.; Nikhil, G.N.; Chitanya, D.N.S.K.; Sinha, P.R.; Ramakrishna, M.; Rao, A.G. Impact of oxides of Nitrogen, Volatile Organic Carbons and Black Carbon emissions on Ozone weekend/weekday variations at a semi arid urban site in Hyderabad. *Aerosol Air Qual. Res.* **2012**, *12*, 662–671. [[CrossRef](#)]
94. Reddy, B.S.K.; Kumar, R.K.; Balakrishnaiah, G.; Rama Gopal, K.; Reddy, R.R.; Ahammed, Y.N.; Narasimhulu, K.; Reddy, S.S.L.; Lal, S. Observational studies on the variations in surface O₃ concentration at Anantapur in southern India. *Atmos. Res.* **2010**, *98*, 125–139. [[CrossRef](#)]
95. Singla, V.; Satsangi, A.; Pachauri, T.; Lakhani, A.; Kumari, K.M. O₃ formation and destruction at a sub-urban site in North Central region of India. *Atmos. Res.* **2011**, *101*, 373–385. [[CrossRef](#)]
96. Debaje, S.; Jeyakumar, S.J. High O₃ at coastal sites in India. *Int. J. Remote Sens.* **2011**, *32*, 993–1015. [[CrossRef](#)]
97. Debaje, S.B.; Kakade, A.D. Surface O₃ variability over western Maharashtra, India. *J. Hazard. Mater.* **2009**, *161*, 686–700. [[CrossRef](#)] [[PubMed](#)]
98. Ghude, D.; Jain, S.L.; Arya, B.C.; Beig, G.; Ahammed, Y.N.; Kumar, A.; Tyagi, B. O₃ in ambient air at a tropical megacity, Delhi: Characteristics, trends and cumulative O₃ exposure indices. *J. Atmos. Chem.* **2008**, *60*, 237–252. [[CrossRef](#)]
99. Beig, G.; Gunthe, S.; Jadhav, D.B. Simultaneous measurements of ozone and its precursors on a diurnal scale at a semi urban site in India. *J. Atmos. Chem.* **2007**, *57*, 239–253. [[CrossRef](#)]
100. Naja, M.; Lal, S.; Chand, D. Diurnal and seasonal variabilities in surface O₃ at a high altitude site Mt Abu (24.60 N, 72.70 E, 1680 m asl) in India. *J. Atmos. Environ.* **2003**, *37*, 4205–4215. [[CrossRef](#)]
101. Naja, M.; Lal, S. Surface O₃ and precursor gases at Gadanki (13.5° N, 79.2° E), a tropical rural site in India. *J. Geophys. Res.* **2002**, *107*, ACH-8. [[CrossRef](#)]
102. Lal, S.; Naja, M.; Subbaraya, B.H. Seasonal variations in surface O₃ and its precursors over an urban site in India. *J. Atmos. Environ.* **2000**, *34*, 2713–2724. [[CrossRef](#)]
103. Sai Krishnaveni, A.; Madhavan, B.L.; Jain, C.D.; Venkat Ratnam, M. Spatial, temporal features and influence of meteorology on PM_{2.5} and O₃ association across urban and rural environments of India. *Atmos. Environ. X* **2024**, *22*, 100265. [[CrossRef](#)]
104. Resmi, C.T.; Fei, Y.; Sarang, S.; Nishanth, T.; Satheesh Kumar, M.K.; Balachandramohan, M.; Manivannan, D.; Hu, J.; Valsaraj, K.T. Variation of trace gases in Kannur town, a coastal South Indian city. *Environ. Chall.* **2021**, *5*, 100336. [[CrossRef](#)]
105. Resmi, C.T.; Nishanth, T.; Satheesh Kumar, M.K.; Balachandramohan, M.; Valsaraj, K.T. Long-term variations of air quality influenced by surface ozone in a coastal site in India: Association with synoptic meteorological conditions with model simulations. *Atmosphere* **2020**, *11*, 193. [[CrossRef](#)]
106. Nair, P.R.; Ajayakumar, R.S.; David, L.M.; Girach, I.A.; Kavitha, M. Decadal changes in surface ozone at the tropical station Thiruvananthapuram (8.542° N, 76.858° E), India: Effects of anthropogenic activities and meteorological variability. *Environ. Sci. Pollut. Res.* **2018**, *25*, 14827–14843. [[CrossRef](#)] [[PubMed](#)]
107. Gopal, R.K.; Lingaswamy, A.P.; Arafath, S.M.; Balakrishnaiah, G.; Kumari, P.S.; Devi, U.K.; Reddy, S.K.N.; Reddy, R.K.B.; Reddy, R.R.; Azeem, A.P.; et al. Seasonal heterogeneity in ozone and its precursors (NO_x) by in-situ and model observations on semi-arid station in Anantapur (A.P.), South India. *J. Atmos. Environ.* **2014**, *84*, 294–306. [[CrossRef](#)]
108. Udayasoorian, C.; Jayabalakrishnan, R.M.; Suguna, A.R.; Venkataramani, S.; Lal, S. Diurnal and seasonal characteristics of ozone and NO_x over a high altitude Western Ghats location in Southern India. *Adv. Appl. Sci. Res.* **2013**, *4*, 309–320.
109. Girach, I.A.; Ojha, N.; Babu, S.S. Ozone chemistry and dynamics at a tropical coastal site impacted by the COVID-19 lockdown. *J. Earth Syst. Sci.* **2021**, *130*, 158. [[CrossRef](#)]
110. David, L.M.; Nair, P.R. Diurnal and seasonal variability of surface ozone and NO_x at a tropical coastal site: Association with mesoscale and synoptic meteorological conditions. *J. Geophys. Res.* **2011**, *116*, D10303. [[CrossRef](#)]
111. Nair, P.R.; Chand, D.; Lal, S.; Modh, K.S.; Naja, M.; Parameswaran, K.; Ravindran, S.; Venkataramani, S. Temporal variations in surface O₃ at Thumba (8.6° N, 77° E)—A tropical coastal site in India. *J. Atmos. Environ.* **2002**, *36*, 603–610. [[CrossRef](#)]

112. Nishanth, T.; Satheesh Kumar, M.K.; Valsaraj, K.T. Variations in surface ozone and NO_x at Kannur: A tropical, coastal site in India. *J. Atmos. Chem.* **2012**, *69*, 101–126. [[CrossRef](#)]
113. Nishanth, T.; Praseed, K.M.; Satheesh Kumar, M.K.; Valsaraj, K.T. Influence of ozone precursors and PM₁₀ on the variation of surface O₃ over Kannur, India. *Atmos. Res.* **2014**, *138*, 112–124. [[CrossRef](#)]
114. Revathy, A.S.; Girach, I.A.; Soni, M.; Ojha, N.; Babu, S.S. Processes governing the surface ozone over a tropical hill station in the Western Ghats. *Atmos. Environ.* **2024**, *319*, 120286. [[CrossRef](#)]
115. Fei, Y.; Dipesh, R.; Lin, H.; Nishanth, T.; Satheesh Kumar, M.K.; Lin, L.; Valsaraj, K.T.; Hu, J. Integrated process analysis retrieval of changes in ground-level ozone and fine particulate matter during the COVID-19 outbreak in the coastal city of Kannur, India. *Environ. Pollut.* **2022**, *307*, 119468. [[CrossRef](#)]
116. Jaffe, D.; Ray, J. Increase in surface ozone at rural sites in the western US. *J. Atmos. Environ.* **2007**, *41*, 5452–5463. [[CrossRef](#)]
117. Camilleri, R.; Vella, A.J. Effect of fireworks on ambient air quality in Malta. *J. Atmos. Environ.* **2010**, *44*, 4521–4527. [[CrossRef](#)]
118. Croteau, G.; Dills, R.; Beaudreau, M.; Davis, M. Emission factors and exposures from ground level pyrotechnics. *J. Atmos. Environ.* **2010**, *44*, 3295–3303. [[CrossRef](#)]
119. Shon, Z.H.; Jeong, J.H.; Kim, Y.K. Characteristics of atmospheric metalliferous particles during large-scale fireworks in Korea. *Adv. Meteorol.* **2015**, *2015*, 3–13. [[CrossRef](#)]
120. Wehner, B.; Weidensohler, A.; Heintzenberg, J. Sub micrometer aerosol sized distributions and mass concentrations of the millennium fireworks 2000 in Leipzig, Germany. *J. Aerosol. Sci.* **2000**, *31*, 1489–1493. [[CrossRef](#)]
121. Attri, A.K.; Kumar, U.; Jain, V.K. Formation of ozone by fireworks. *Nature* **2001**, *411*, 1015. [[CrossRef](#)]
122. Ganguly, N.D.; Tzani, C.G.; Philippopoulos, K.; Deligiorgi, D.; Ganguly, N.D.; Tzani, C.G.; Philippopoulos, K.; Deligiorgi, D. Analysis of a severe air pollution episode in India during Diwali festival—A nationwide approach. *Atmósfera* **2019**, *32*, 225–236. [[CrossRef](#)]
123. Mandal, J.; Chanda, A.; Samanta, S. Air pollution in three megacities of India during the Diwali festival amidst COVID-19 pandemic. *Sustain. Cities Soc.* **2022**, *76*, 103504. [[CrossRef](#)]
124. Saxena, P.; Srivastava, A.; Verma, S.; Singh, L.; Sonwani, S. Analysis of Atmospheric Pollutants During Fireworks Festival ‘Diwali’ at a Residential Site Delhi in India. In *Measurement, Analysis and Remediation of Environmental Pollutants. Energy, Environment, and Sustainability*; Gupta, T., Singh, S., Rajput, P., Agarwal, A., Eds.; Springer: Singapore, 2020. [[CrossRef](#)]
125. Garg, A.; Sharma, P.; Beig, G.; Ghosh, C. Temporal Mount in Air Pollutants Allied with Religious Fiesta: Diwali, Festival of Lights. In *Emerging Issues in Ecology and Environmental Science: Case Studies from India*; SpringerBriefs in Environmental Science; Springer: Berlin/Heidelberg, Germany, 2018; pp. 11–25. [[CrossRef](#)]
126. Ambade, B. The air pollution during Diwali festival by the burning of fireworks in Jamshedpur city, India. *Urban Clim.* **2018**, *26*, 149–160. [[CrossRef](#)]
127. Peshin, S.K.; Sinha, P.; Bisht, A. Impact of Diwali firework emissions on air quality of New Delhi, India during 2013–2015. *Mausam* **2017**, *68*, 111–118. [[CrossRef](#)]
128. Resmi, C.T.; Nishanth, T.; Satheesh Kumar, M.K.; Balachandramohan, M.; Valsaraj, K.T. Assessment of extreme fireworks episode in a coastal city of Southern India- Kannur as a Case Study. In *Atmospheric Processes, Phenomena and Its Related Extremities*; Springer Nature Publications: Singapore, 2022; ISBN 978-981-16-7727-4. [[CrossRef](#)]
129. Resmi, C.T.; Nishanth, T.; Satheesh Kumar, M.K.; Balachandramohan, M.; Valsaraj, K.T. Temporal changes in air quality during a festival season in Kannur, India. *Atmosphere* **2019**, *10*, 137. [[CrossRef](#)]
130. Nishanth, T.; Praseed, K.M.; Rathnakaran, K.; Satheesh Kumar, M.K.; RaviKrishna, R.; Valsaraj, K.T. Atmospheric pollution in a semi-urban, coastal region in India following festival seasons. *J. Atmos. Environ.* **2012**, *47*, 295–306. [[CrossRef](#)]
131. Wilson, W.E.; Westenberg, A.A. Study of the reaction of hydroxyl radical with methane by quantitative ESR. *Symp. (Int.) Combust.* **1967**, *11*, 1143–1150. [[CrossRef](#)]
132. Dutta, D.; Kumar, V.P.; Ratnam, M.V.; Mohammad, S.; Kumar, M.C.A.; Rao, P.V.; Rahaman, K. Response of tropical lower atmosphere to annular solar eclipse of 15 January 2010. *J. Atmos. Sol. Terr. Phys.* **2011**, *73*, 1907–1914. [[CrossRef](#)]
133. Jenan, R.; Dammalage, T.L.; Panda, S.K. Ionospheric total electron content response to September-2017 geomagnetic storm and December-2019 annular solar eclipse over Sri Lankan region. *Acta Astronaut.* **2021**, *180*, 575–587. [[CrossRef](#)]
134. Kurdyaeva, Y.; Borchevkina, O.; Karpov, I.; Kshevetskii, S. Thermospheric disturbances caused by the propagation of acoustic-gravity waves from the lower atmosphere during a solar eclipse. *Advanc. Space Res.* **2021**, *68*, 1390–1400. [[CrossRef](#)]
135. Rao, S.S.; Chakraborty, M.; Singh, A.K. A study on TEC reduction during the tail phase of the 21st June 2020 annular solar eclipse. *Adv. Space Res.* **2021**, *67*, 1948–1957. [[CrossRef](#)]
136. Senturk, E.; Adil, M.A.; Saqib, M. Ionospheric total electron content response to annular solar eclipse on June 21, 2020. *Adv. Space Res.* **2021**, *67*, 1937–1947. [[CrossRef](#)]
137. Gerasopoulos, E.; Zerefos, C.S.; Tzagouri, I.; Founda, D.; Amiridis, V.; Bais, A.F.; Belehaki, A.; Christou, N.; Economou, G.; Kanakidou, M.; et al. The total solar eclipse of March 2006: Overview. *Atmos. Chem. Phys.* **2008**, *8*, 5205–5220. [[CrossRef](#)]
138. Chakraborty, D.K.; Shah, N.C.; Pandya, K.V. Fluctuation in ozone column over Ahmedabad during the solar eclipse of 24 October 1995. *Geophys. Res. Lett.* **1997**, *24*, 3001–3003. [[CrossRef](#)]
139. Lal, S.; Subbaraya, B.H. Solar eclipse induced variations in mesospheric ozone concentrations. *Adv. Space Res.* **1983**, *2*, 205. [[CrossRef](#)]

140. Venkat Ratnam, M.; Basha, G.; Roja Raman, M.; Kumar Mehta, S.; Murthy, K.; Jayaraman, A. Unusual enhancement in temperature and ozone vertical distribution in the lower stratosphere observed over Gadanki, India, following the 15 January 2010 annular eclipse. *Geophys. Res. Lett.* **2011**, *38*, 1–5. [[CrossRef](#)]
141. Zanis, P.; Katragkou, E.; Kanakidou, M.; Psiloglou, B.E.; Karathanasis, S.; Vrekoussis, M.; Gerasopoulos, E.; Markakis, K.; Poupkou, A.; Amiridis, V.; et al. Effects on surface atmospheric photo-oxidants over Greece during the total solar eclipse event of 29 March 2006. *Atmos. Chem. Phys.* **2007**, *7*, 6061–6073. [[CrossRef](#)]
142. Manchanda, R.K.; Sinha, P.R.; Sreenivasan, S.; Trivedi, D.B.; Kapardhi, B.V.N.; Kumar, B.S.; Kumar, P.R.; Satyaprakash, U.; Rao, V.N. In-situ measurements of vertical structure of O₃ during the solar eclipse of 15 January 2010. *J. Atmos. Sol. Terr. Phys.* **2012**, *84*, 88–100. [[CrossRef](#)]
143. Anoop, P.; Muhsin, M.; Shebin, J.; Aiswarya, S.; Arun, P.T.; Deepa, V.; Ravi, V. Trace pollutant fluctuations observed in Calicut city, India, during the annular solar eclipse on 26 December 2019. *Atmos. Pollut. Res.* **2020**, *11*, 2049–2055.
144. Jain, C.D.; Ratnam, M.V.; Madhavan, B.L. Direct and indirect photochemical impacts on the trace gases observed during the solar eclipse over a tropical rural location. *J. Atmos. Sol. -Terr. Phys.* **2020**, *211*, 105451. [[CrossRef](#)]
145. Resmi, C.T.; Nishanth, T.; Satheesh Kumar, M.K.; Balachandramohan, M.; Valsaraj, K.T. Annular solar eclipse on 26 December 2019 and its effect on trace pollutant concentrations and meteorological parameters in Kannur, India: A coastal city. *Asian J. Atmos. Environ.* **2020**, *14*, 290–307. [[CrossRef](#)]
146. Nishanth, T.; Ojha, N.; Satheesh Kumar, M.K.; Naja, M. Influence of solar eclipse of 15 January 2010 on surface O₃. *J. Atmos. Environ.* **2011**, *45*, 1752–1758. [[CrossRef](#)]
147. Sharma, S.K.; Mandal, T.K.; Arya, B.C.; Saxena, M.; Shukla, D.K.; Mukherjee, A.; Bhatnagar, R.P.; Nath, S.; Yadav, S.; Gautam, R.; et al. Effects of solar eclipse on 15 January on the surface O₃, NO, NO₂, NH₃, CO mixing ratio and the meteorological parameters at Thiruvananthapuram India. *Ann. Geophys.* **2010**, *28*, 1199–1205. [[CrossRef](#)]
148. Akhil Raj, S.T.; Ratnam, M.V. Ozone vertical distribution during the solar eclipse of 26 December 2019 over Gadanki: Role of background dynamics. *Atmos. Pollut. Res.* **2021**, *12*, 101116. [[CrossRef](#)]

Disclaimer/Publisher’s Note: The statements, opinions and data contained in all publications are solely those of the individual author(s) and contributor(s) and not of MDPI and/or the editor(s). MDPI and/or the editor(s) disclaim responsibility for any injury to people or property resulting from any ideas, methods, instructions or products referred to in the content.